Diagnostic Assessments and Modeling Strategies Appropriate to the Development of Weather and Climate Models

Donald R. Johnson

Emeritus Professor, U of Wisconsin

NCEP Special Project Scientist, NOAA

Modeling and diagnostic strategies employed in the development and employment of the UW Hybrid Isentropic Model including some which have been utilized at NCEP will be briefly reviewed. Within an emphasis on the importance of long range transport and ensuring reversibility, results will be presented which illustrate the relevance of these considerations. The aim of the review and results presented, however, will be: 1) to raise key issues faced in advancing accuracies in the simulation of weather and climate and, 2) to foster discussion on strategies to isolate the strengths and current limitations of weather and climate models within a unified modeling endeavor envisaged as a key component of the Earth System Modeling Framework.

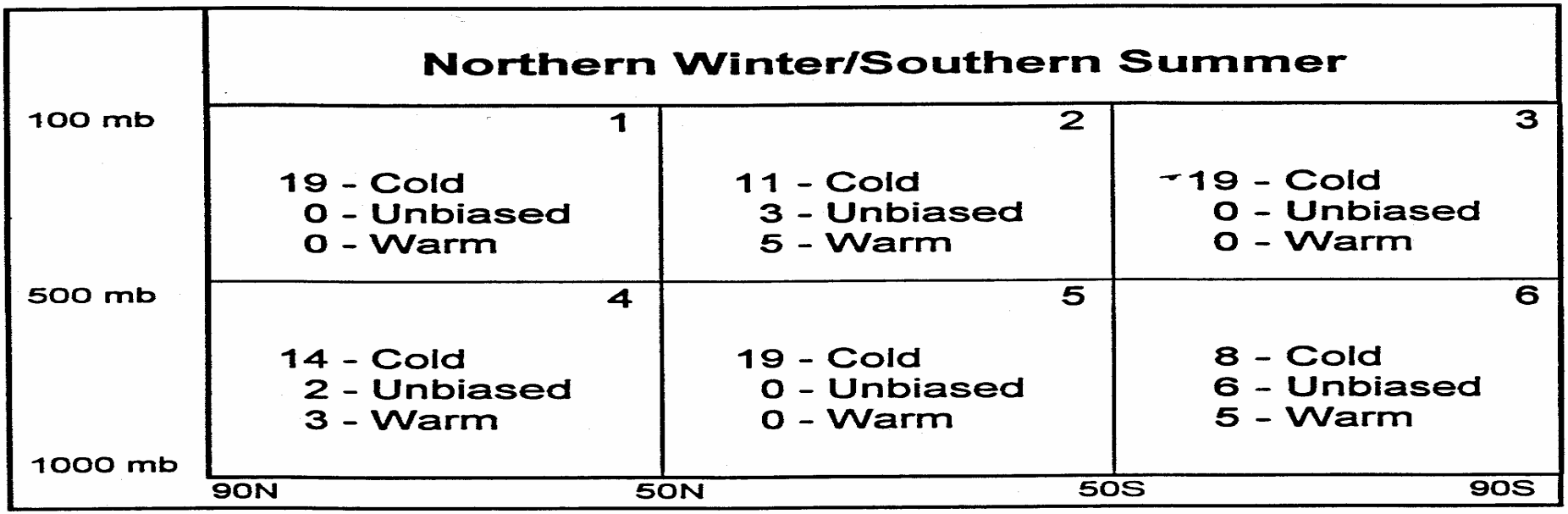

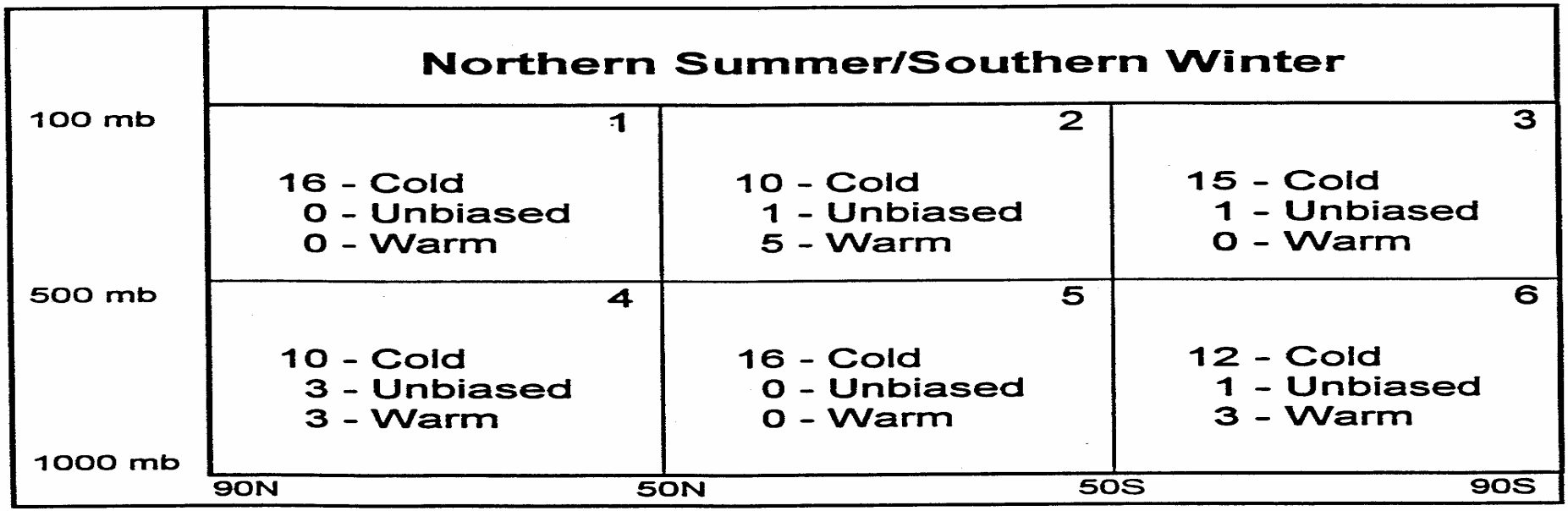

Figure 1: A summarized tabulation of the number of climate model simulated temperatures classified predominately cold, warm or unbiased relative to observations within the six regions indicated. This tabulation was summarized from Table 4 of the WMO Report, "An Intercomparison of the Climate Simulated by 14 Atmospheric General Circulations Models" (Boer et al. 1991).

Isentropic Efficiency Factor

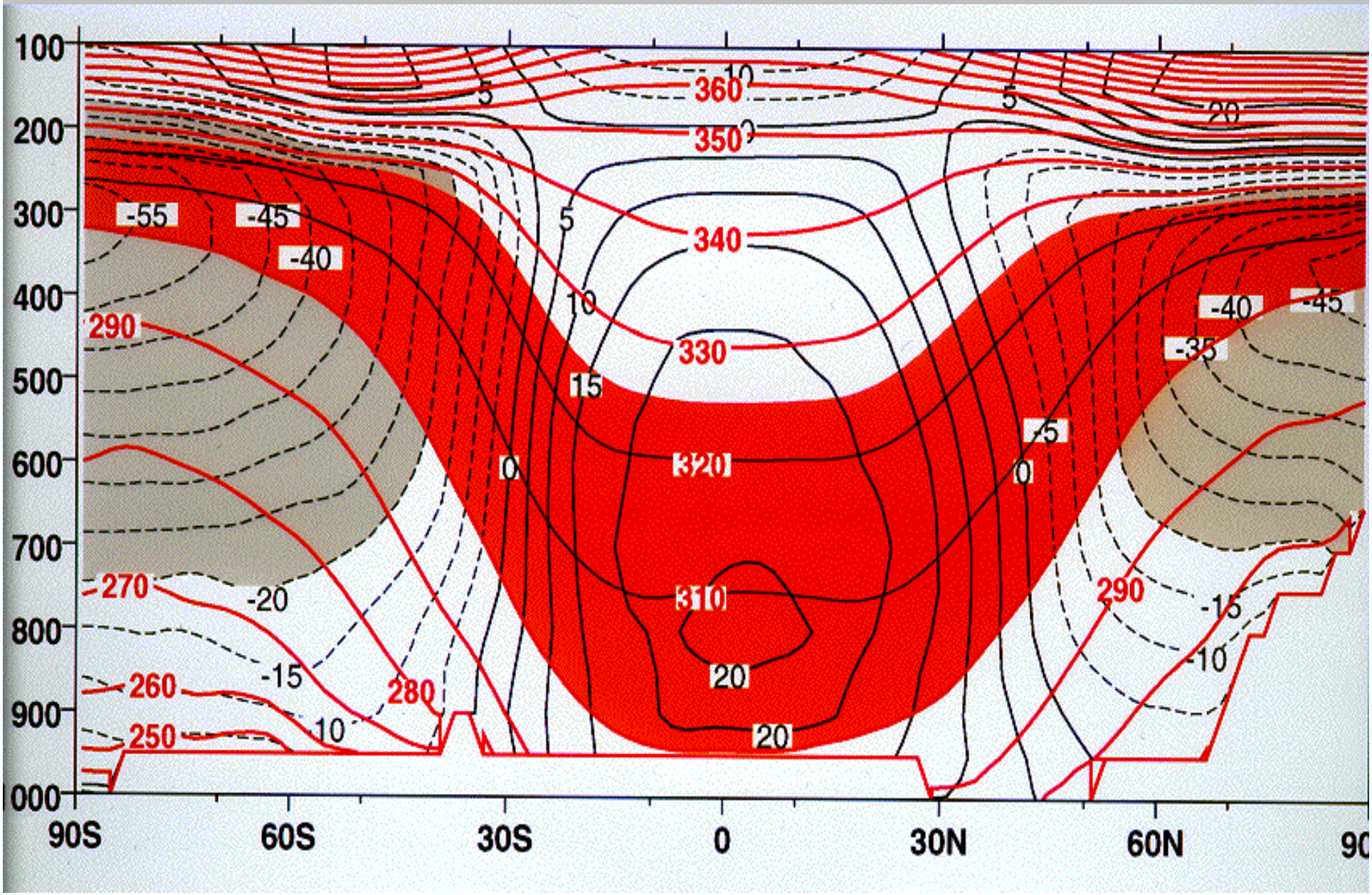

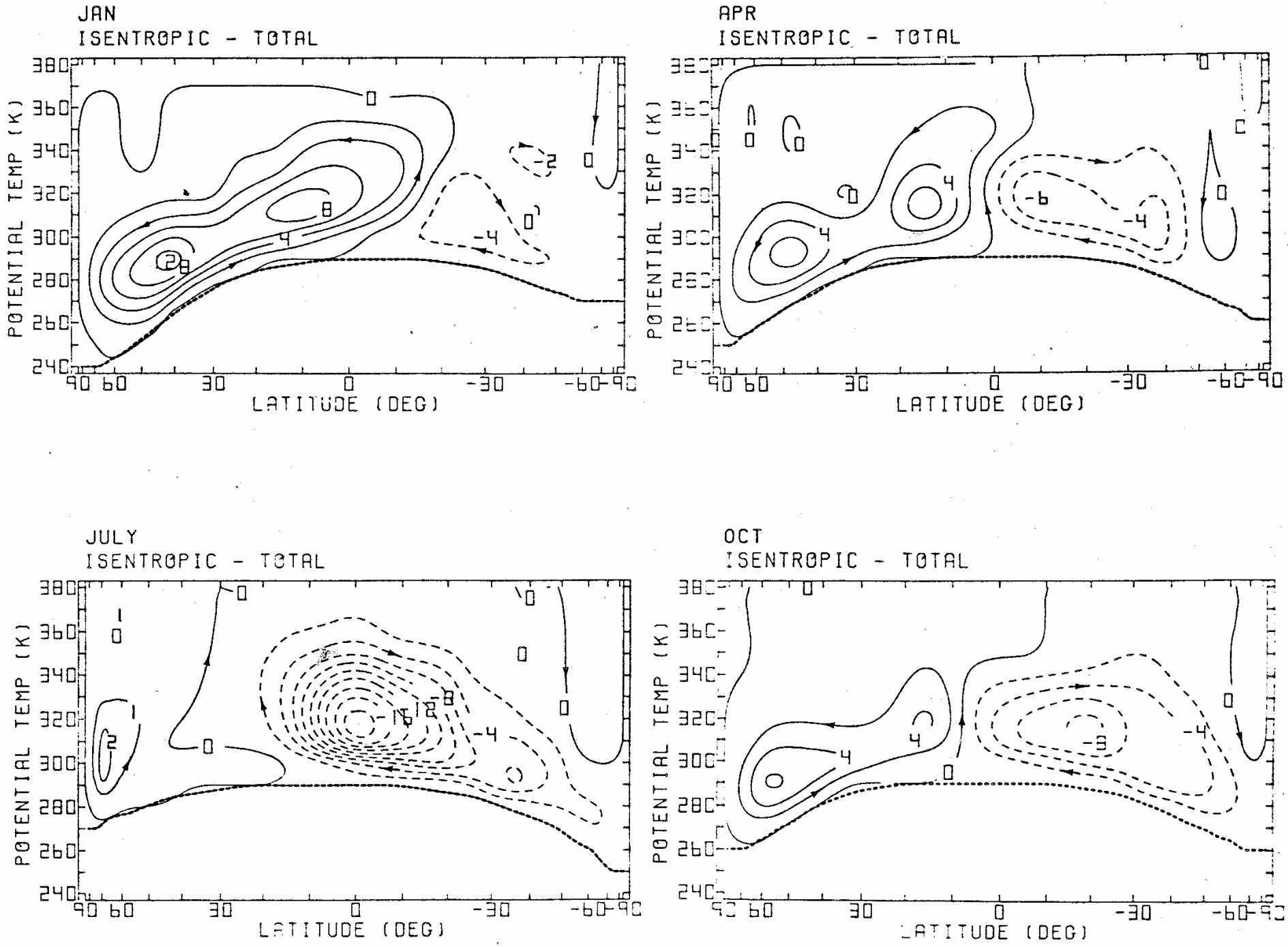
JAN
ISENTROPIC - TOTAL
APR
ISENTROPIC - TOTAL
JULY
ISENTROPIC - TOTAL
OCT
ISENTROPIC - TOTAL
POTENTIAL TEMP (K)
LATITUDE (DEG)
380
360
340
320
300
280
260
240
90 60
30
0
-30
-60
-90

Mintz's perspective of a thermodynamic cycle embedded in the westerlies

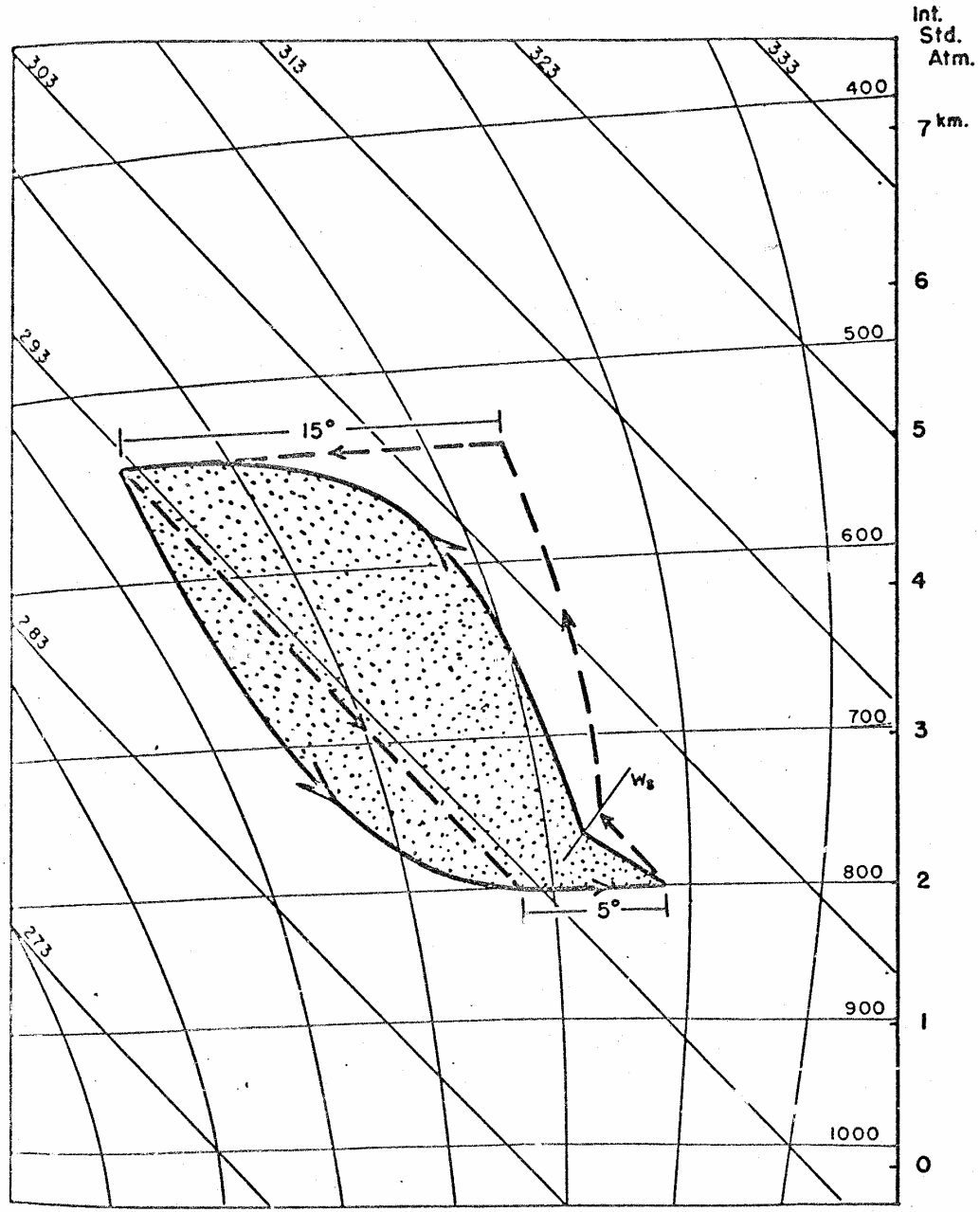

Fig. 6--Image curve of a symmetrical westerly helical trajectory in the tephigram

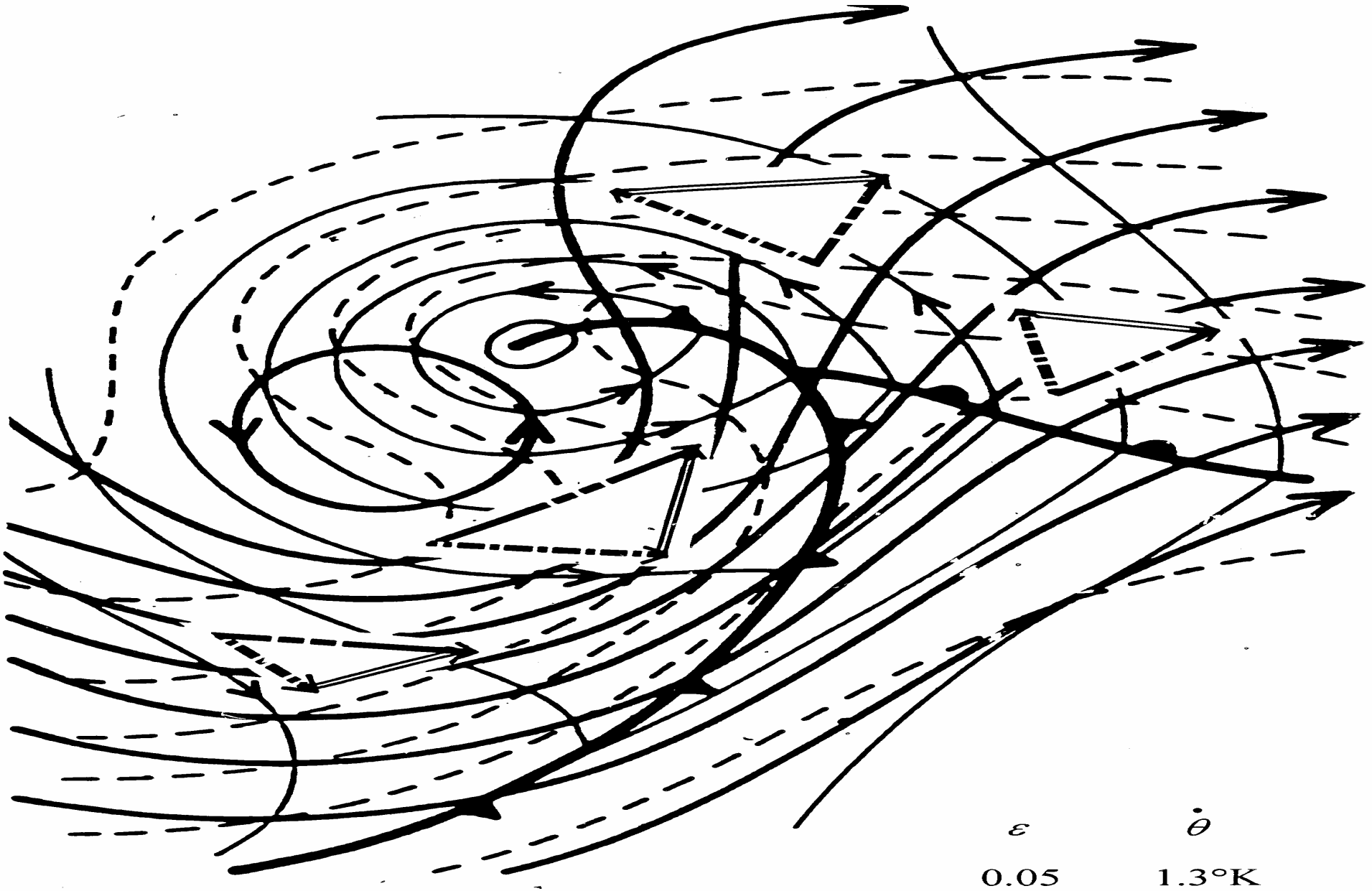

ε	$\dot{\theta}$
0.05	1.3°K
0.1	1.76°
0.2	3.16°

Modeling and Analysis of the Earth's Hydrologic Cycle

Donald R. Johnson Tom H. Zapotocny Todd K. Schaack Allen J. Lenzen

Space Science and Engineering Center, University of Wisconsin – Madison

Introduction

A key aim of this research is to further understanding of global water vapor and inert trace constituent transport in relation to climate change through analysis of simulations produced by the global University of Wisconsin (UW) hybrid isentropic-sigma coordinate models. Advancing the accuracy of the simulation of water substances, aerosols, chemical constituents, potential vorticity and stratospheric-tropospheric exchange are all critical to DOE's goal of accurate climate prediction on decadal to centennial time scales and assessing anthropogenic effects. Research has established that simulations of the transport of water vapor, and inert and chemical constituents are remarkably more accurate in hybrid isentropic coordinate models than in corresponding sigma coordinate models.

Primary Objectives:

- Advance the modeling of climate change by developing an isentropic hybrid model for global and regional climate simulations.
- Advance the understanding of physical processes involving water substances and the transport of trace constituents.
- Diagnostically examine the limits of global and regional climate predictability imposed by inherent limitations in the simulation of trace constituent transport, hydrologic processes and cloud life-cycles.

Key Findings:

- The results demonstrate the viability of the UW θ–η model for long term climate integration, numerical weather prediction and chemistry.
- The studies document that no insurmountable barriers exist for realistic simulations of the climate state with the hybrid vertical coordinate.
- Experiments reported here demonstrate a high degree of numerical accuracy for the UW θ–η model in simulating reversibility and potential vorticity transport over 10 day period that corresponds to the global residence time of water vapor.
- The UW hybrid θ–η model simulates seasonally varying and interannual climate scales realistically, including monsoonal circulations associated with El Nino/La Nina events.

Selected References

Schaack, T. K., T. H. Zapotocny, A. J. Lenzen and D. R. Johnson, 2004: Global climate simulation with the University of Wisconsin global hybrid isentropic coordinate model. Accepted for publication in *Journal of Climate*.

Johnson, D. R., A. J. Lenzen, T. H. Zapotocny and T. K. Schaack, 2002: Entropy, numerical uncertainties and modeling of atmospheric hydrologic processes: Part B. *J. Climate*, 15, 1777-1804.

Johnson, D. R., A. J. Lenzen, T. H. Zapotocny, and T. K. Schaack, 2000: Numerical uncertainties in the simulation of reversible isentropic processes and entropy conservation. *J. Climate*, 13, 3860-3884.

Johnson, D. R., 2000: Entropy, the Lorenz Energy Cycle and Climate. In *"General Circulation Model Development: Past, Present and Future"* (D. A. Randall, ed.), Academic Press, pp. 659-720.

Reames, F. M. and T. H. Zapotocny, 1999a: Inert trace constituent transport in sigma and hybrid isentropic-sigma models. Part I: Nine advection algorithms. *Mon. Wea. Rev.*, 127, 173-187.

Reames, F. M. and T. H. Zapotocny, 1999b: Inert trace constituent transport in sigma and hybrid isentropic-sigma models. Part II: Twelve semi-Lagrangian algorithms. *Mon. Wea. Rev.*, 127, 188-200.

Johnson, D. R., 1997: On the "General Coldness of Climate Models" and the Second Law: Implications for Modeling the Earth System. *J. Climate*, 10, 2826-2846.

Zapotocny, T. H., A. J. Lenzen, D. R. Johnson, F. M. Reames, and T. K. Schaack, 1997a: A comparison of inert trace constituent transport between the University of Wisconsin isentropic-sigma model and the NCAR community climate model. *Mon. Wea. Rev.*, 125, 120-142.

Zapotocny, T. H., D. R. Johnson, T. K. Schaack, A. J. Lenzen, F. M. Reames, and P. A. Politowicz, 1997b: Simulations of Joint Distributions of Equivalent Potential Temperature and an Inert Trace Constituent in the UW θ–σ Model and CCM2. *Geophys. Res. Let.*, 24, 865-868.

Zapotocny, T. H., A. J. Lenzen, D. R. Johnson, F. M. Reames, P. A. Politowicz, and T. K. Schaack, 1996: Joint distributions of potential vorticity and inert trace constituent in CCM2 and UW θ–σ model simulations. *Geophys. Res. Let.*, 23, 2525-2528.

Zapotocny, T. H., D. R. Johnson, and F. M. Reames, 1994: Development and initial test of the University of Wisconsin global isentropic-sigma model. *Mon. Wea. Rev.*, 122, 2160-2178.

A. Design of Model Vertical Coordinate

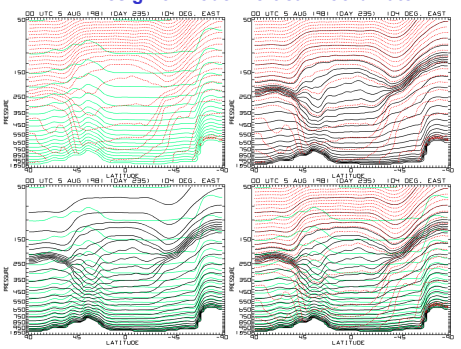

Fig. 1. Schematic of meridional cross sections along 104E for 05 August 1981. The red lines represent potential temperature; the black lines represent UW θ–η model surfaces; the green lines represent scaled sigma model surfaces.

B. Accuracy Analysis of Transport and Reversibility

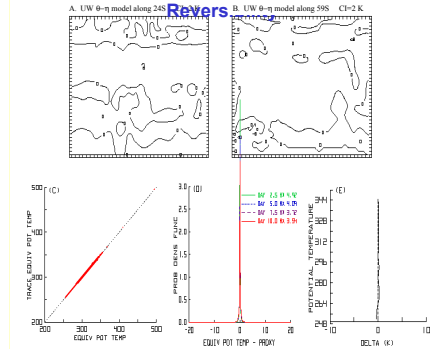

Fig. 2. The top two panels show zonal cross sections of the difference between θe and trace θe (CI=2 K) from the UW θ–η model at day 10. Panel C shows a bivariate distribution of θe and trace θe at day 10, panel D shows a relative frequency distribution of simulated differences between θe and trace θe at days 2.5, 5, 7.5 and 10, and panel E shows a vertical profile of the differences at day 10.

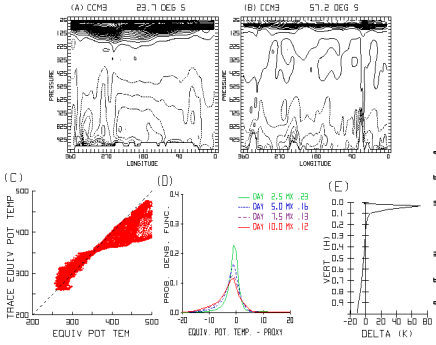

Fig. 3. Same as Fig. 2 except for CCM3 running at T42 horizontal resolution.

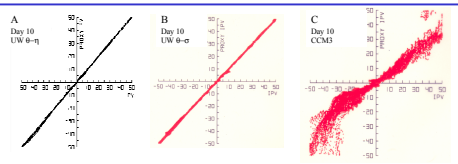

Fig. 4. Bivariate distributions of ozone and a proxy trace ozone. The "Day 10" distributions from the UW θ–η model, UW θ–σ model, and T42 CCM3 are shown in panels (A)-(C) respectively.

Table 1. Results from analysis of variance globally for the difference of equivalent potential temperature minus its trace (θe-t θe) and three components at day 10. Units of variance are the square of Kelvin temperature (K^2). Quantity in parenthesis is the RMS temperature difference (±K).

UW Hybrid Model				
UW θ–σ	0.70(0.84)	0.23(0.48)	0.13(0.35)	1.05 (1.03)
UW θ–η	0.12 (0.35)	0.01 (.10)	0.03 (.16)	0.16 (0.40)
CCM2 and CCM3				
	$S_G(\delta^*)$	$S_G(\bar{\delta}^*)$	$S_G(\bar{\delta})$	$S_G(\delta)$
CCM3	37.45 (6.12)	195.77 (13.99)	0.02 (.15)	233.24 (15.27)
CCM3/2	27.88 (5.28)	0.09 (0.30)	0.03 (0.16)	28.00 (5.29)
CM2(all spectral)	10.83 (3.29)	2.12 (1.46)	15.03 (3.88)	27.98 (5.29)
CCM3(all semi-Lagrangian)	3.41 (1.85)	0.64 (0.79)	0.03 (0.16)	4.08 (2.02)
CCM3				
CCM3 Standard	37.45 (6.12)	195.77 (13.99)	0.02 (.15)	233.24 (15.27)
CCM3 Modified	5.93 (2.44)	0.25 (.50)	0.01 (.09)	6.19 (2.49)

The first three columns respectively list the variances of 1) the differences about the area mean difference, 2) area mean differences about the grand mean difference and 3) the variance of the grand mean difference. The last column lists the total variance of the differences.

C. UW q-h Climate Simulations

Table 2. A comparison of annually averaged fields from the 13-year UW θ–η model climate simulation to observed values. Observational estimates are from a summary by Hack et al. 1998.

Field	Observed	UW q-h model
All-sky OLR (W m^{-2})	234.8	238.4
Clear sky OLR (W m^{-2})	266.0	266.3
Total cloud forcing (W m^{-2})	-950	-114
Longwave cloud forcing (W m^{-2})	29.2	27.9
Shortwave cloud forcing (W m^{-2})	-48.2	-41.3
Total Cloud fraction (%)	52.3 ±0.5	60.7
Precipitable water (mm)	24.7	22.8
Precipitation (mm day^{-1})	2.7	3.1
Latent heat flux (W m^{-2})	78.0	88.9
Sensible heat flux (W m^{-2})	20.0	19.3

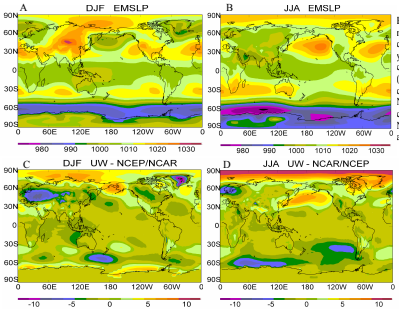

Fig. 5. The time averaged mean sea-level pressure distributions from the 13 year UW θ–η model climate simulation for DJF (A) and JJA (B) as well as differences from the NCEP/NCAR reanalysis climatology (UW-NCEP/NCAR) for DJF (C) and JJA (D).

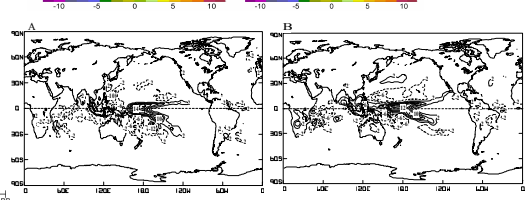

Fig. 6. Global distributions of the difference (DJF 1987-88 minus DJF 1988-89) between seasonally average precipitation for DJF 1987-88 and DJF 1988-89 (mm/day) from the (A) Xie and Arkin (1997) climatology and (B) UW θ–η model climate simulation.

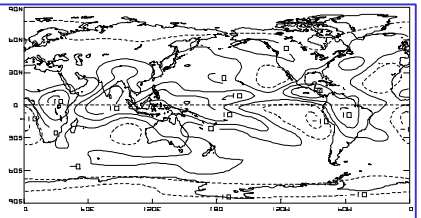

Fig. 7. The distribution of annual vertically averaged heating (10^{-1} K/Day) from the last 13 years of a 14 year climate run with UW θ–η model.

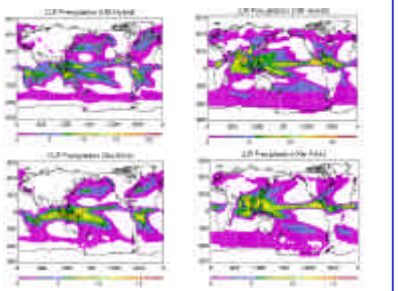

Fig. 8. The time averaged distributions of precipitation (mm/day) from the 13 year UW θ–η model climate simulation for DJF (A) and JJA (B) and from the Xie and Arkin precipitation climatology for 1979-99 for DJF (C) and JJA (D).

D. NCEP and NASA Collaborative Studies

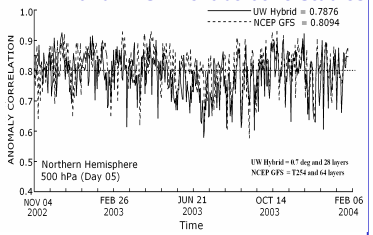

Fig. 9. Fifteen month record of Anomaly Correlation from the UW θ–η model and NCEP Global Forecast System.

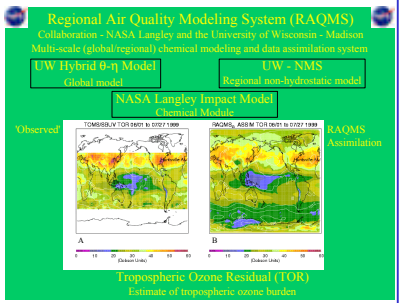

Fig 10. The UW hybrid model forms the global component of the RAQMS data assimilation system. Figure B shows tropospheric ozone burden (DU) for June-July 1999 from the RAQMS assimilation while Fig. A is the satellite observed estimate.

A Statement of Principle Concerning Model Diversity and Diagnostics in Relation to the Earth System Modeling Framework (ESMF)

"Within the context of an umbrella for model diagnostics and validation, lets us strive to develop an assessment strategy and capability for advancing global models and the underlying science that is independent of the vested interests and developers of model, whether they be in the government, academic or private sectors. At the same time, the effort should also ensure the mutual interests and activities of the major centers and their scientists in a community effort that isolates deficiencies and shortcomings of global models while advancing modeling accuracies and understanding of global and regional modeling of weather and climate".

Several Underlying Considerations Concerning NOAA's involvement in the ESMF

The following are several underlying considerations aimed to facilitate NOAA's development of weather and climate models under the unified modeling effort envisaged within the ESMF as prepared by Donald R. Johnson, NCEP Special Project Scientist in response to Louis Uccellini's request as the Director of NCEP:

- The agreement that "model diversity within a community framework is required for progress in both weather and climate models" is predicated on the premise that no single model or approach to modeling the weather climate state at this time or in the foreseeable future has achieved the level of accuracy needed for weather and climate prediction.

- Strategies should focus on ascertaining the strengths and weaknesses of models in relation to advancing NOAA's capabilities for weather and climate prediction broadly defined.
- The underlying issue is how through collaborative utilization of the ESMF and working partnerships can NOAA and the larger scientific community advance understanding and accuracies for weather and climate prediction.
- Advancing understanding and prediction of weather and of climate are complementary to each other in implementing an environmental forecasting capability in NOAA that serves the nation's larger interests.
- Within the effort to advance weather and climate prediction for their own purposes and also to mutually complement each other, there must be recognition on the part of the science community, theoreticians, modelers, diagnosticians, and operational forecasters that all have a stake and need to contribute to this effort.
- The challenge then is how to ensure the active engagement of not only those within NOAA including ESMF partners, but also the larger scientific community.

For those who focus on the capabilities of global models to simulate monsoons, regional climate and medium range weather prediction and those who recognize the fundamental importance of water, moist thermodynamic processes, cloudiness and its related impact of radiation and surface energy exchange, there should be common agreement that the scientific challenges in modeling weather and climate are one and the same.

While the focus on carbon and global warming lies somewhat outside of the focus on medium range weather and seasonal climate forecasts, there is the emerging relevance of aerosols, the biosphere and related biogeochemical processes, diurnally varying land and surface boundary conditions and other processes being brought to the forefront that links all. As such, advancing accuracies in the simulation of weather and climate in the coming decade must be viewed as common challenge, particularly as attention is given to implementing an environmental forecasting capability that serves the nation's larger interests.

1. Strategies to assess numerical accuracies of global models utilizing assimilated data as initial conditions:

a. Pure error differences of potential temperature, equivalent potential temperature, and potential vorticity in relation to appropriate conservation with and without moist convective parameterization for differing resolutions, numerics and orders of numerical accuracies, etc., examined in the form of scatter diagrams, empirical pdfs and profiles of systematic biases.

b. Global and regional analysis of variance of pure error differences including determination of systematic biases and component variances---zonal, horizontal, vertical and global.

c. Expansion of the variance of the pure differences, say V(g-tg), yields the sum of the variances V(g) and V(tg) minus two times the covariance Cov(g,tg).

d. Temporal and spatial integrity of filamentary transport of trace constituents and conservation of extremum utilizing proxy initial state constituent conditions consisting of vertically invariant zonal ring and circular symmetric normal distributions as well as other specified distributions.

e. Integrity of transport of water, chemical and aerosol constituents including appropriate conservation in relation to chemical species, families and process interaction.

A challenge common to weather, climate and seasonal numerical prediction is the need to simulate accurately reversible isentropic processes in combination with transport and sources of energy and entropy. A means to study model accuracy is to determine its capability to simulate the appropriate conservation of potential and equivalent potential temperature as surrogates of dry and moist entropy under reversible adiabatic processes in which clouds form, evaporate and precipitate.

An NCAR Reviewers Comment

It is doubtful that strict global conservation of energy and entropy by a numerical scheme plays a significant role in weather prediction. The advantage of center difference schemes like Arakawa and Lamb (1977) in conserving energy and entropy are often over-stated while its shortcomings (e.g., numerical instability near poles; degradation in vorticity advection in divergent flows which results in poor correlation between potential vorticity and passive tracers) being ignored. All models need sub-grid damping mechanisms. How this can be achieved can be very different among models. It should be noted that even the Arakawa and Lamb scheme needs artificial smoothing/filtering (in time and in space) renders all GCMs effectively non-energy conserving and irreversible. In standard CCM3 the total energy is nearly conserved because, 1) the lost kinetic energy due to hyper-viscosity is added back to the thermodynamic equation and also due in part, 2) a lucky cancel-lation between the energy conserving errors in dynamics and physics.

An underlying issue to be examined regarding reversibility is to determine to what degree if any can the appropriate conservation of potential vorticity and dry and moist entropy be disregarded in the simulation of hydrologic and chemical processes for weather and climate

Bivariate distributions of potential vorticity and the trace potential vorticity as determined by the strategy 0f pure error differences from stimulations by the UW Theta-Eta Model and CCM3

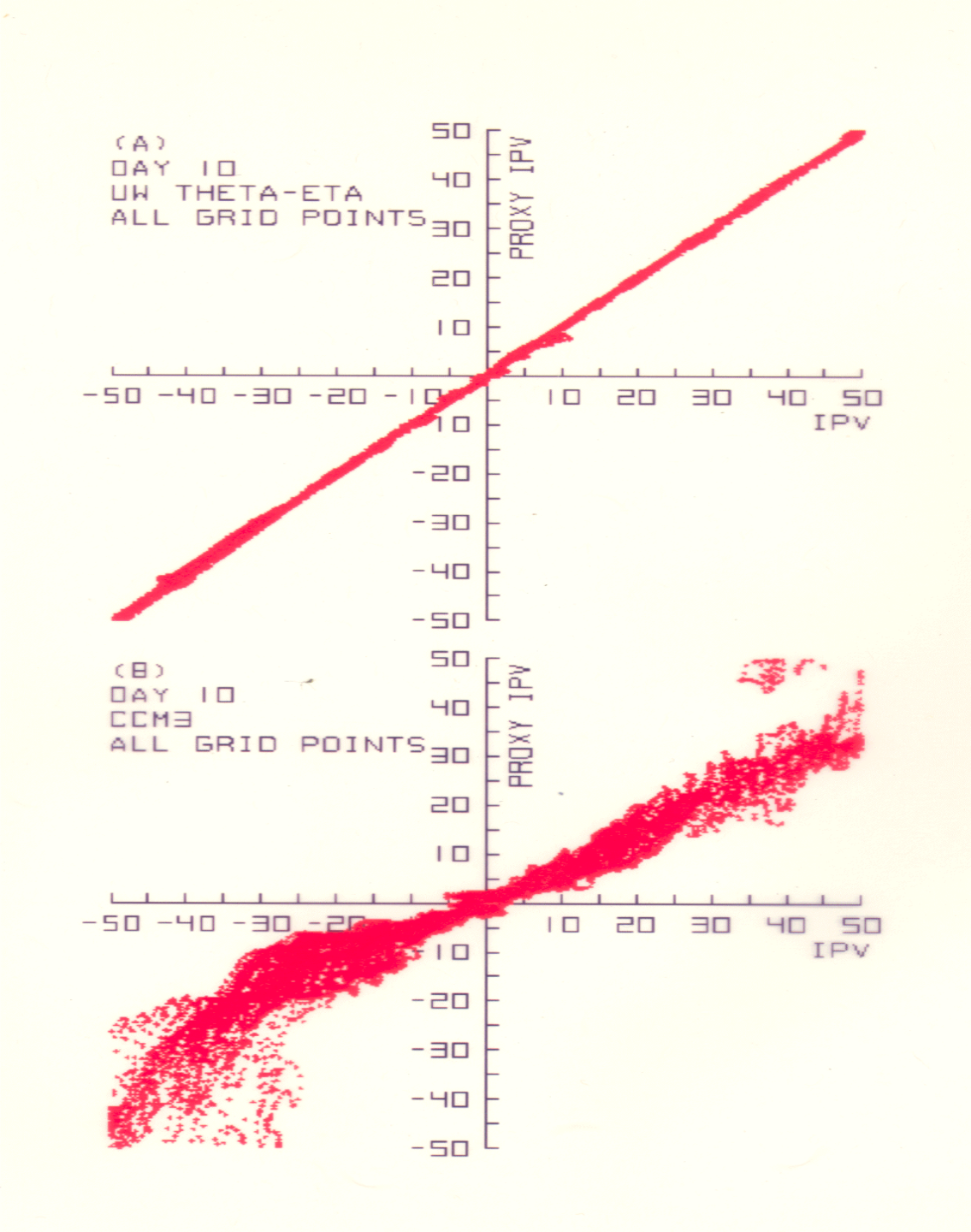

Conservation of Equivalent Potential Temperature - II

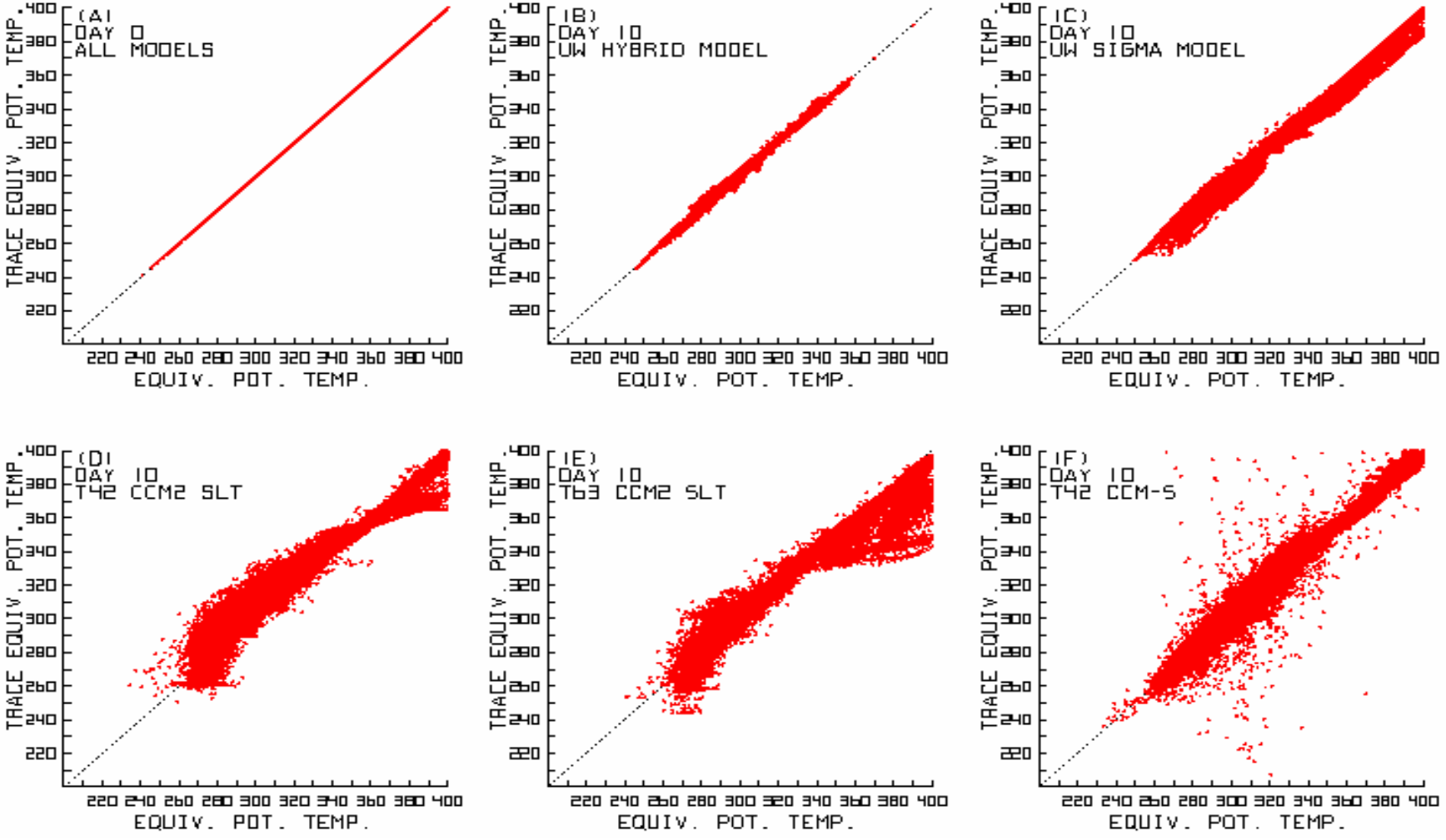

Bivariate Scatter and Relative Frequency Distributions and Vertical Profile of Mean Differences

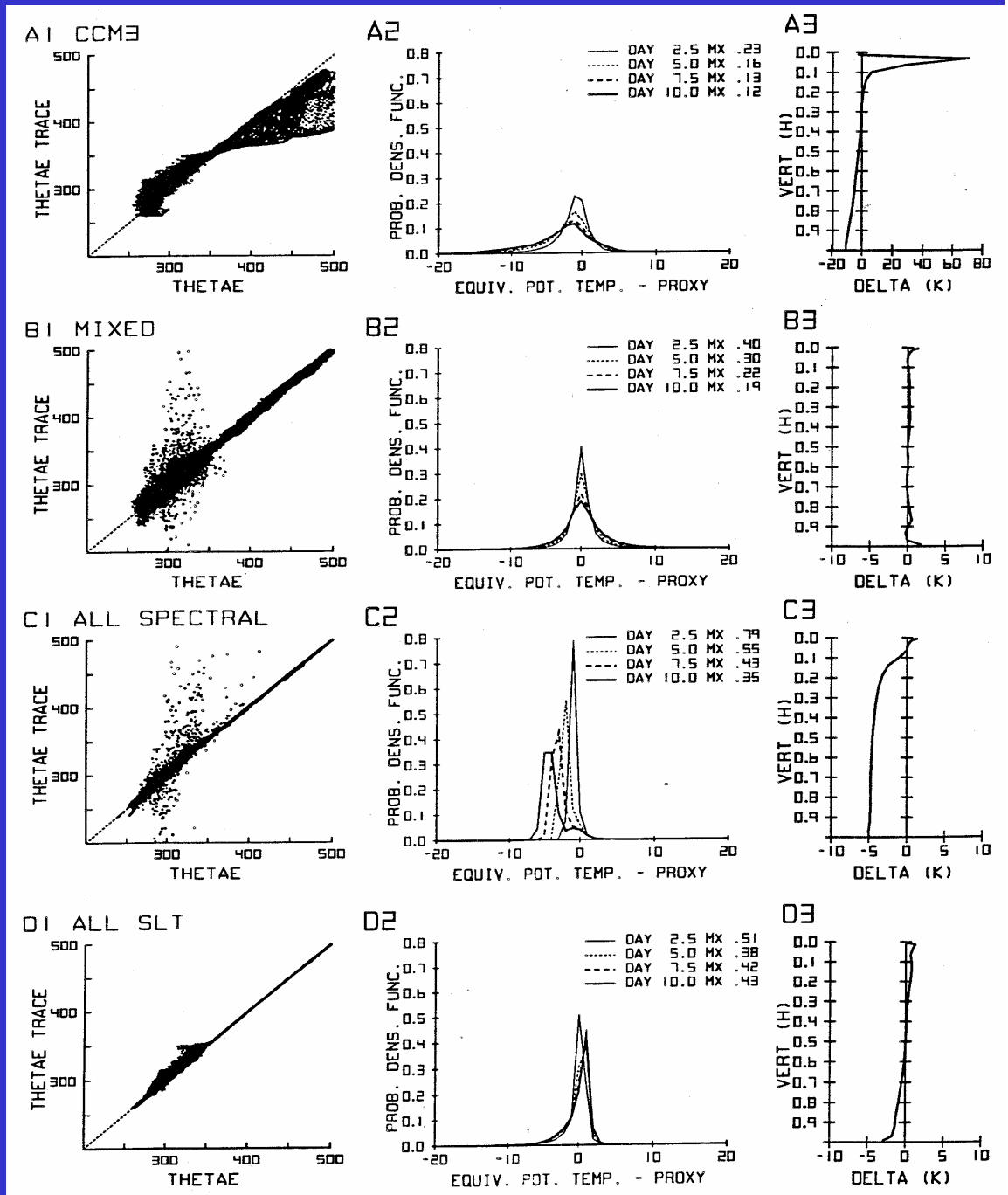

Relative Frequency Distributions of Simulated Differences

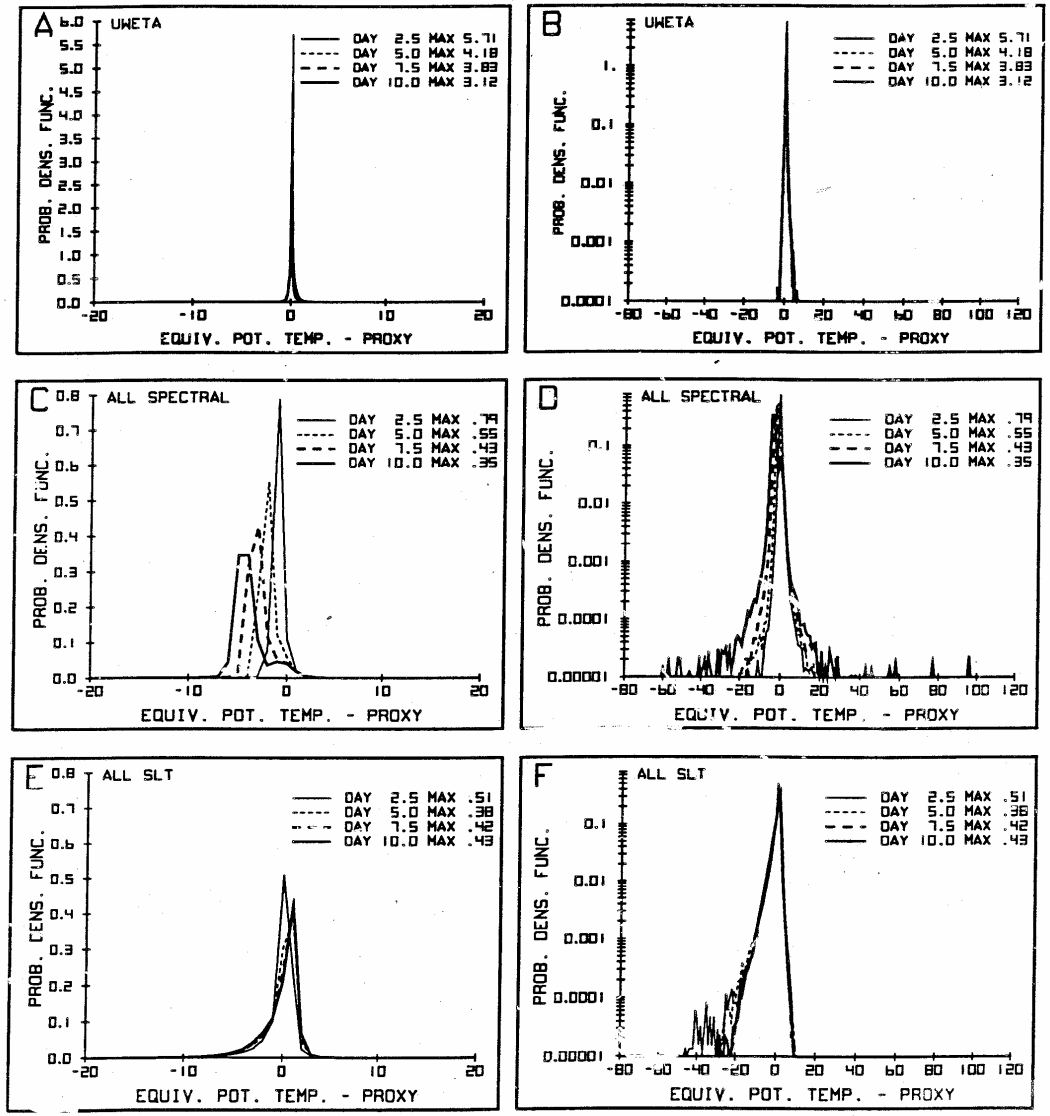

Fig. 1 Empirical relative frequency distributions of simulated differences of equivalent potential temperature θ_e (K) and its proxy $t\theta_e$ (K) for days 2.5, 5, 7.5 and 10. Panels A and B portray results from the UW $\theta-\eta$ model, C and D for the CCM2 all Eulerian spectral experiment and E and F are for the CCM3 all semi-Lagrangian experiment. Vertical axes on the left are scaled linearly, while the vertical axes on the right are scaled logarithmically to retain larger outliers. With bins interval of 0.1 K for the UW $\theta-\eta$ model differences and 1.0 K for the CCM2/3, the magnitude of the maximum are not directly comparable. Recall that sum of the product of the ordinate and the bin interval equals unity.

Relative Frequency Distributions for UW θ-η Model Level by Level

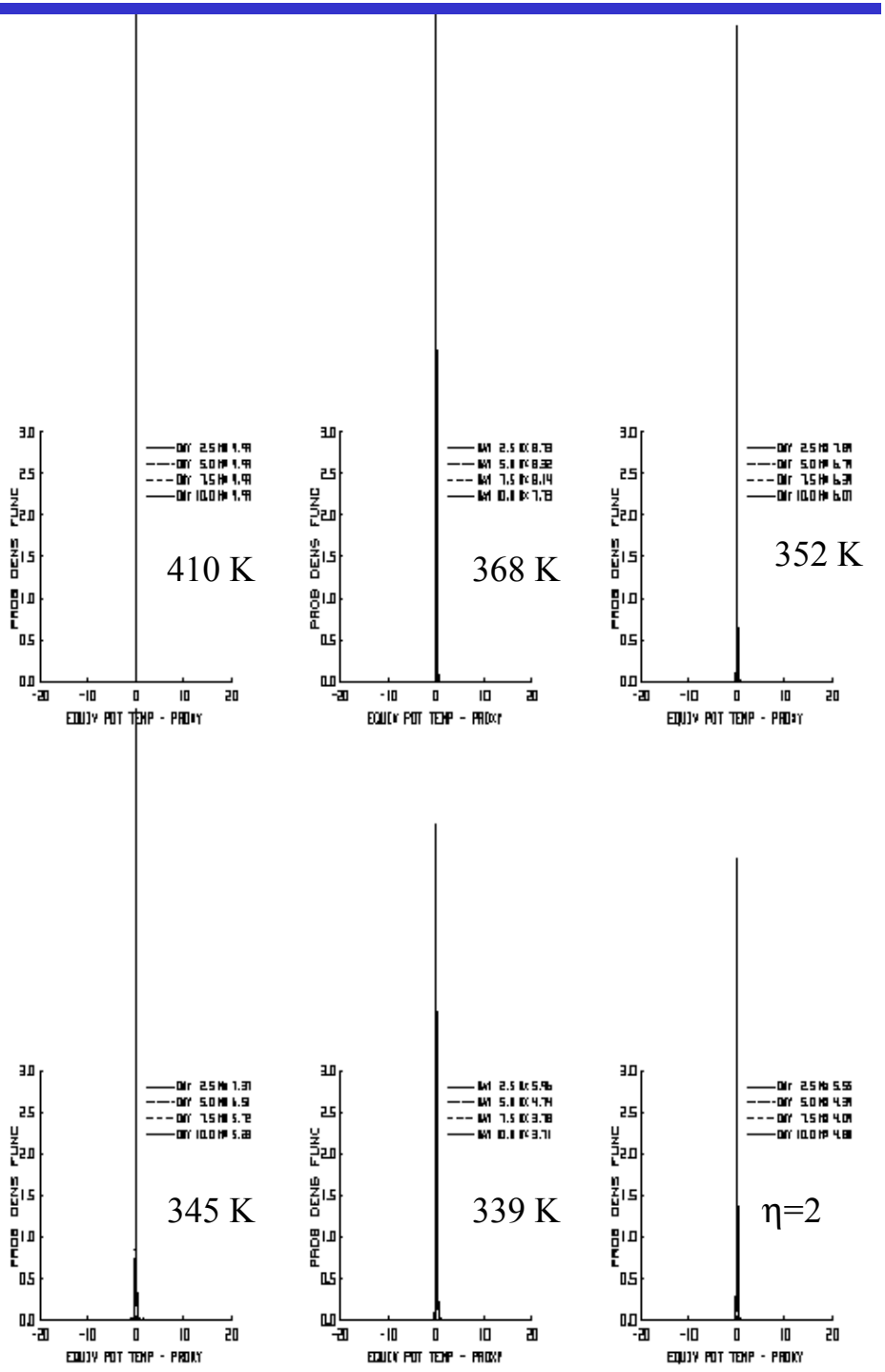

Relative Frequency Distributions for UW θ-η Model Level by Level

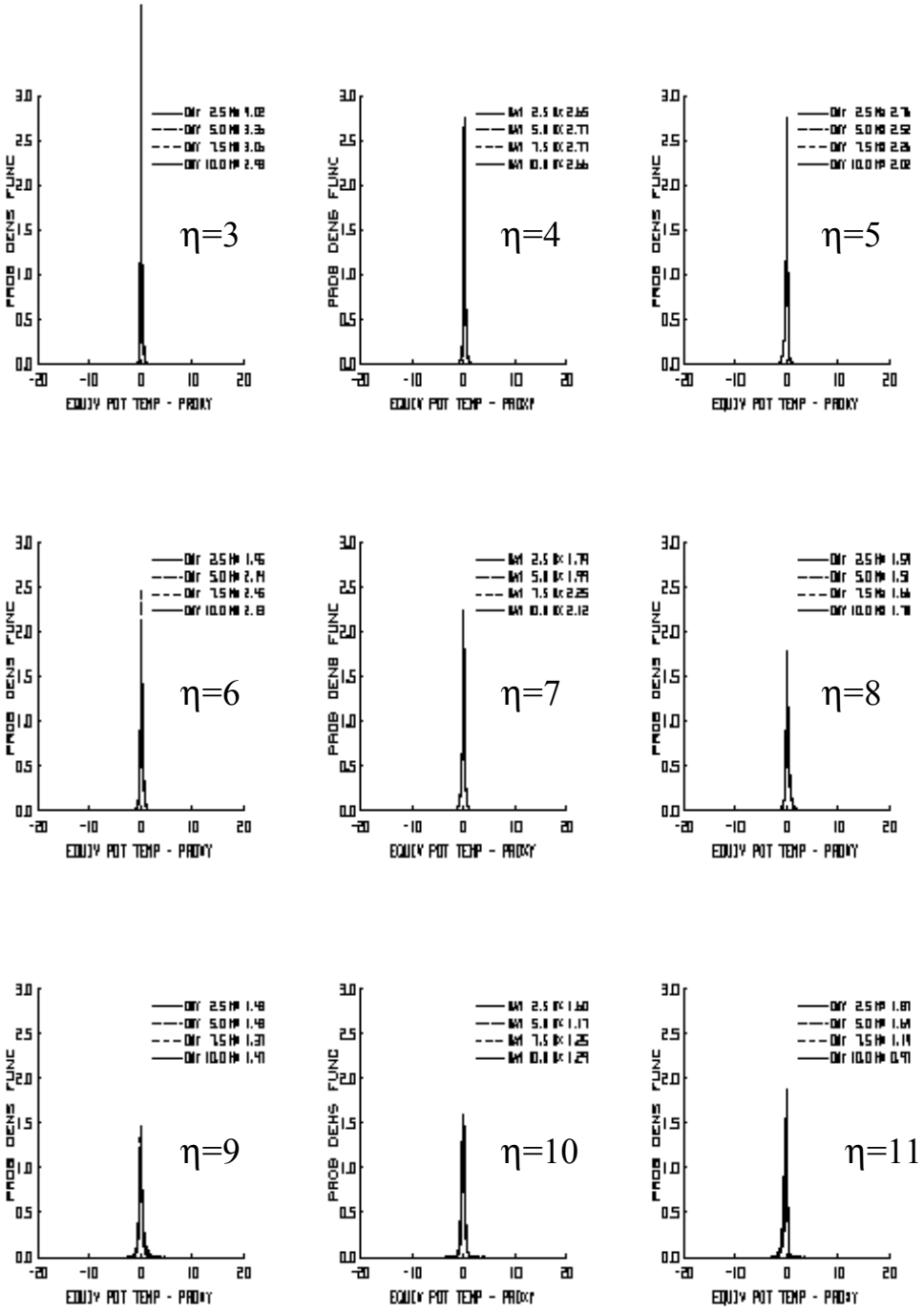

Relative frequency distributions for days 2.5, 5.0, 7.5 and 10.0 for four different versions of CCM at the 4.3H level

CCM3

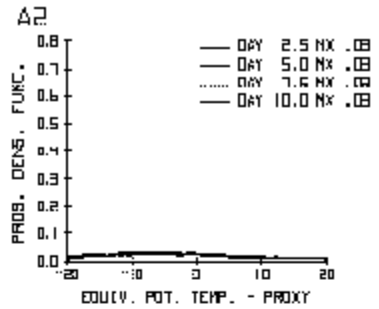

CCM2/3 MIXED

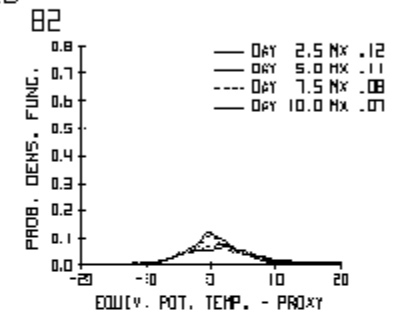

CCM2 ALL EULERIAN SPECTRAL

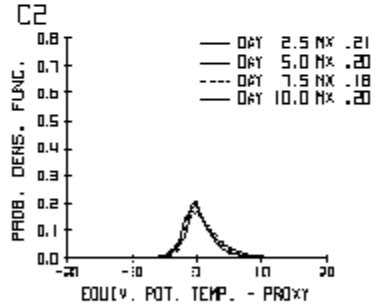

4.3H

CCM3 ALL SLT

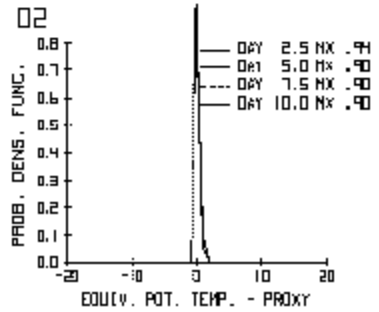

Relative frequency distributions for days 2.5, 5.0, 7.5 and 10.0 for four different versions of CCM at the 970.4H level

CCM3

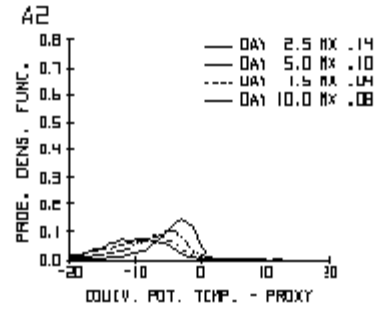

CCM2/3 MIXED

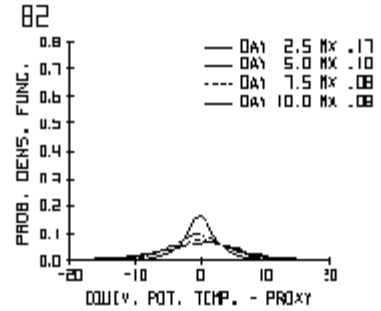

CCM2 A_L EULERIAN SPECTRAL

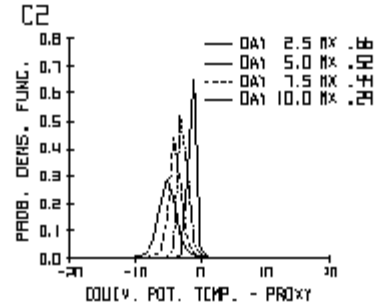

970.4H

CCM3 A_L SLT

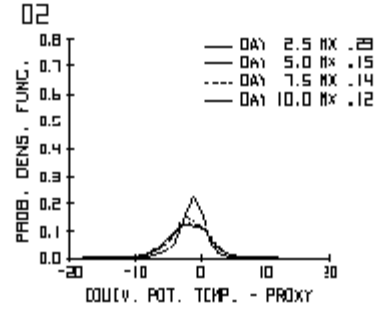

Results from Analysis of Variance Globally for the Difference of Equivalent Potential Temperature Minus its Trace (θ_e-tθ_e) and three components at day 10

CCM2 and CCM3

	$S_G(\delta^*)$	$S_G(\hat{\delta}^*)$	$S_G(\hat{\hat{\delta}})$	$S_G(\delta)$
CCM3	37.45 (6.12)	195.77 (13.99)	0.02 (.15)	233.24 (15.27)
CCM3/2	27.88 (5.28)	0.09 (0.30)	0.03 (0.16)	28.00 (5.29)
CM2(all spectral)	10.83 (3.29)	2.12 (1.46)	15.03 (3.88)	27.98 (5.29)
CCM3(all semi-Lagrangian)	3.41 (1.85)	0.64 (0.79)	0.03 (0.16)	4.08 (2.02)

CCM3

CCM3 Standard	37.45 (6.12)	195.77 (13.99)	0.02 (.15)	233.24 (15.27)
CCM3 Modified	5.93 (2.44)	0.25 (.50)	0.01 (.09)	6.19 (2.49)

UW Hybrid Model

UW $\theta-\sigma$	0.70(0.84)	0.23(0.48)	0.13(0.35)	1.05 (1.03)
UW $\theta-\eta$	0.12 (0.35)	0.01 (.10)	0.03 (.16)	0.16 (0.40)

Units of variance are the square of Kelvin temperature (K^2). Units of quantity in parenthesis as the square root of the variance (standard deviation) are Kelvin temperature ($\pm$ K).

Rectangular and allied distibutions

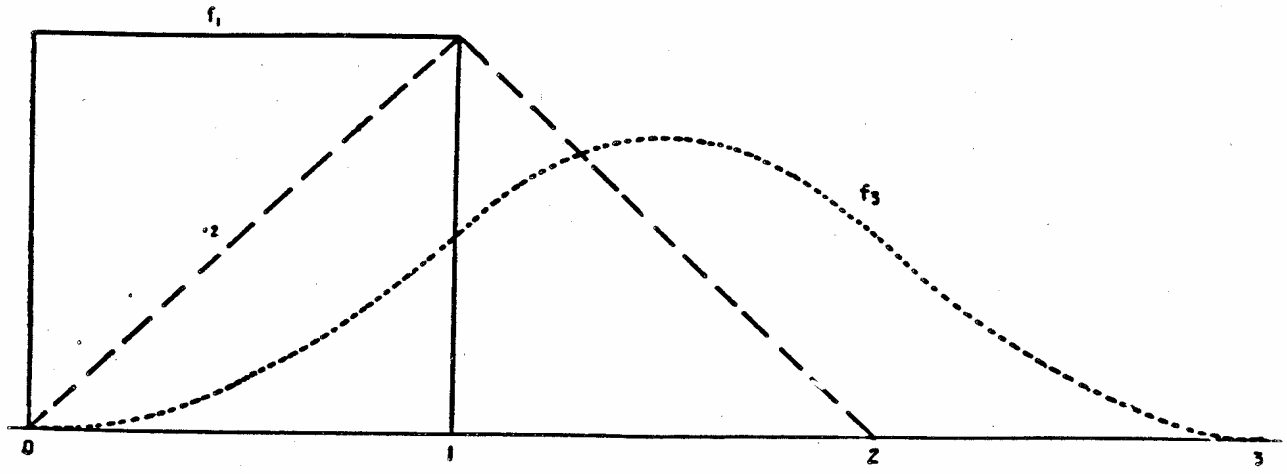

Fig. 21. Rectangular and allied distributions.

The expression of $f_2(x)$ given above may be written in the form

$$f_2(x) = 1 - |1 - x|, \qquad (0 < x < 2).$$

This fr. f., and any fr. f. obtained from it by a linear transformation, is sometimes said to define a *triangular distribution*.

Day 10

Less Horizontal Diffusion

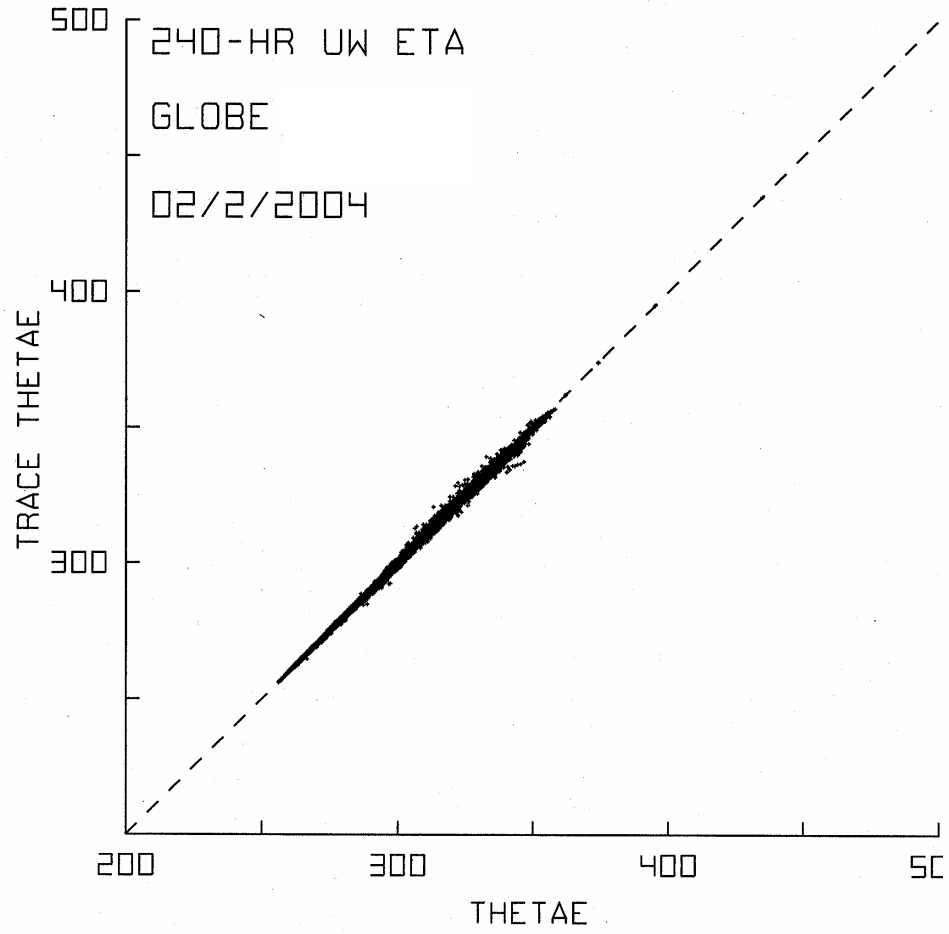

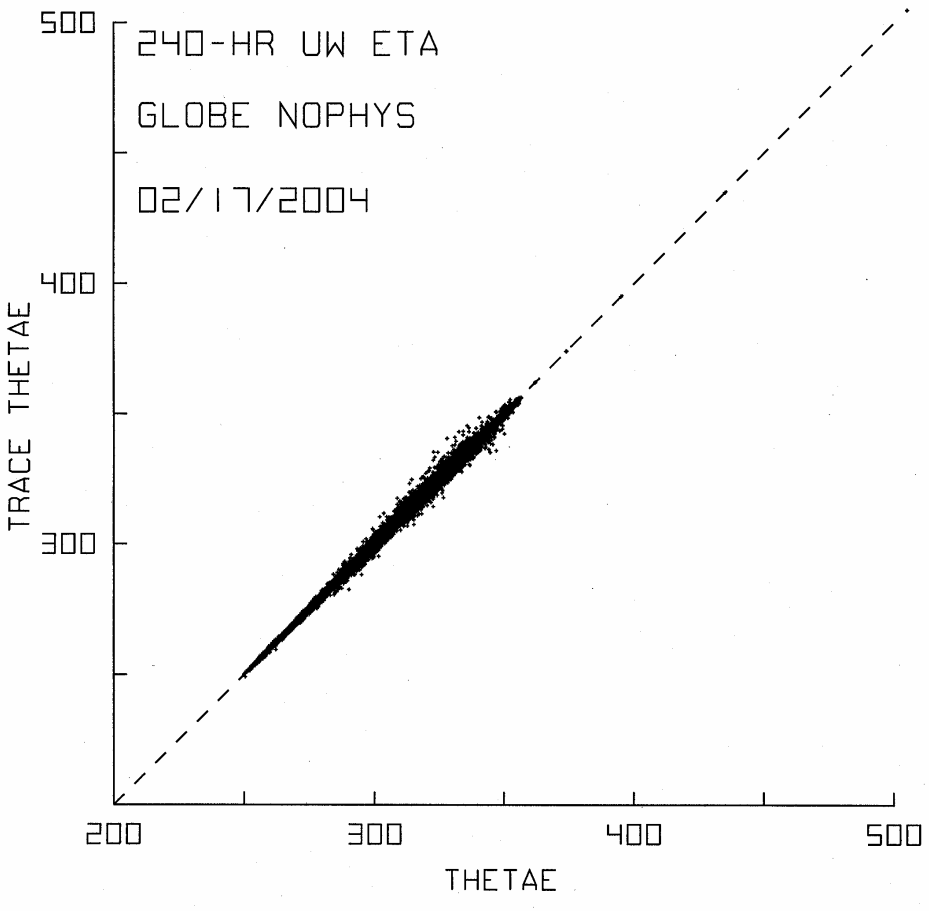

Day 10

Convective and large scale condensation plus radiation

Source/sink of θ_e entered in trace equation

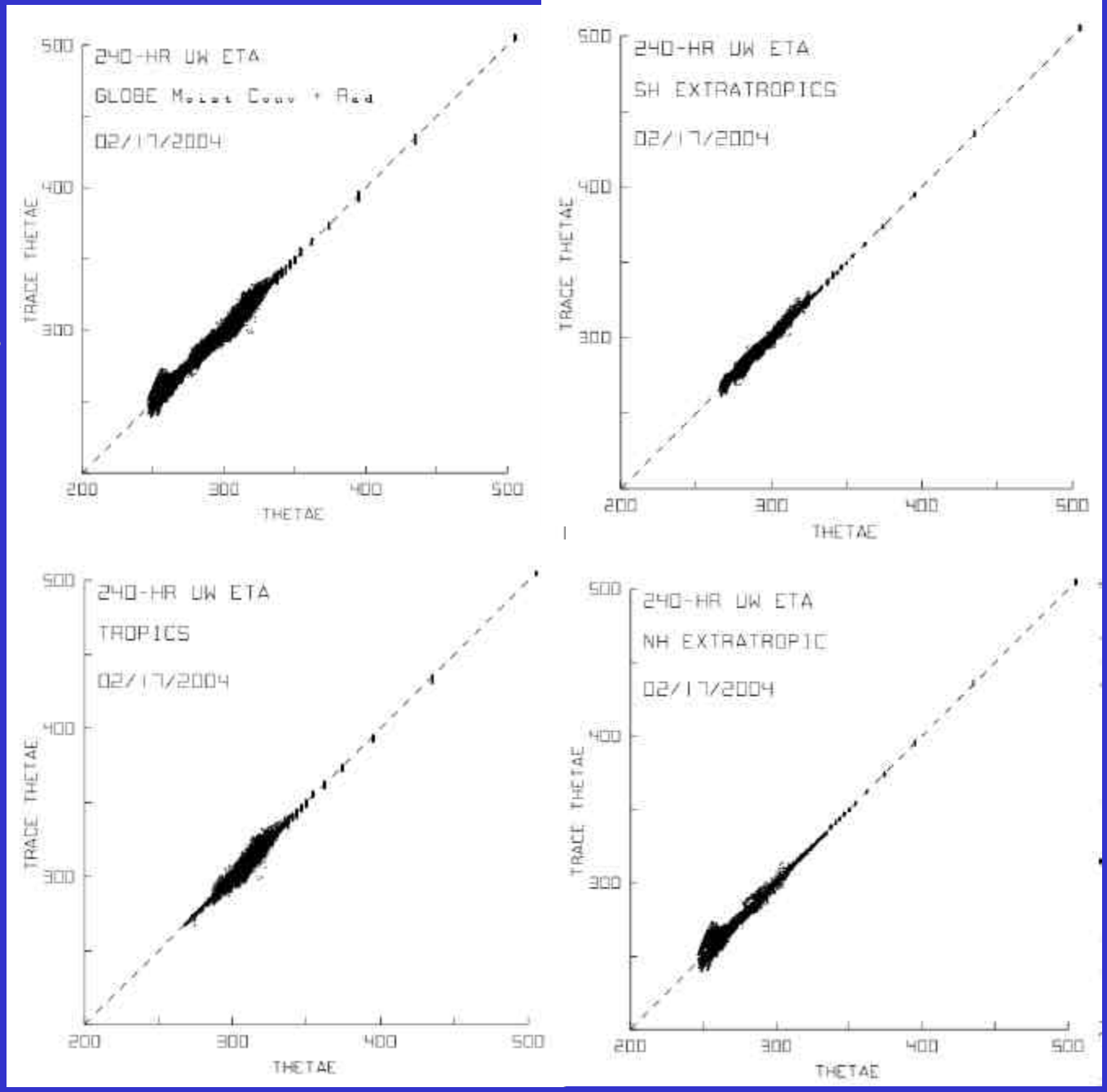

Day 10

Source/sink of θ_e entered in trace equation

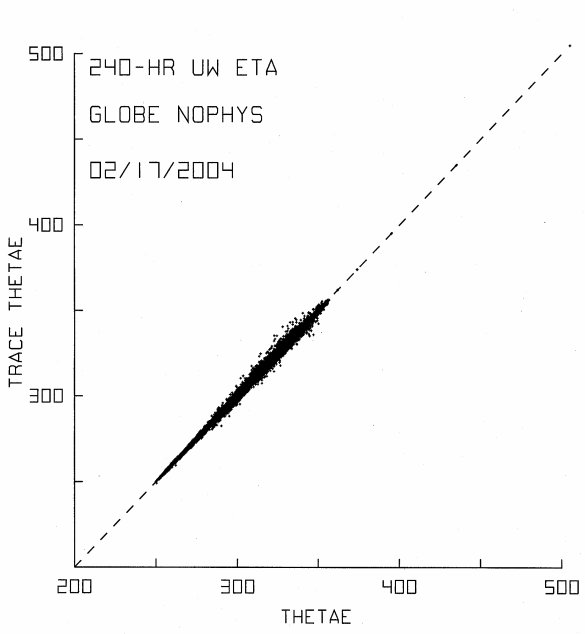

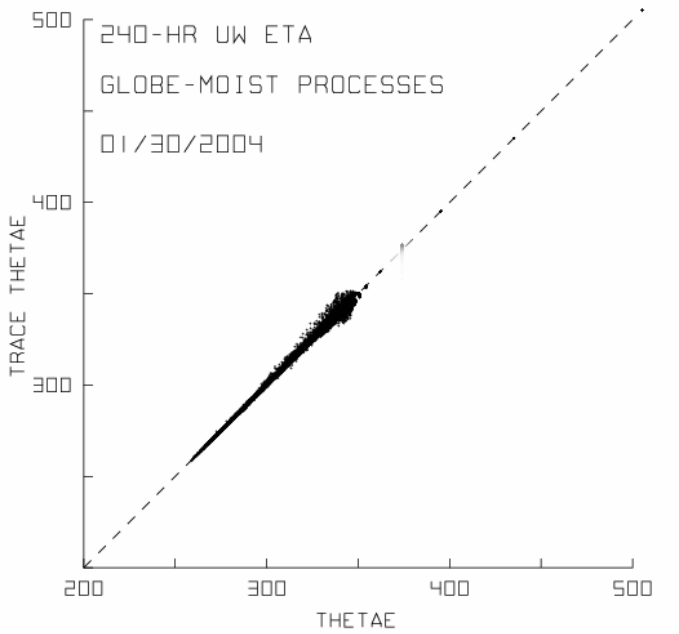

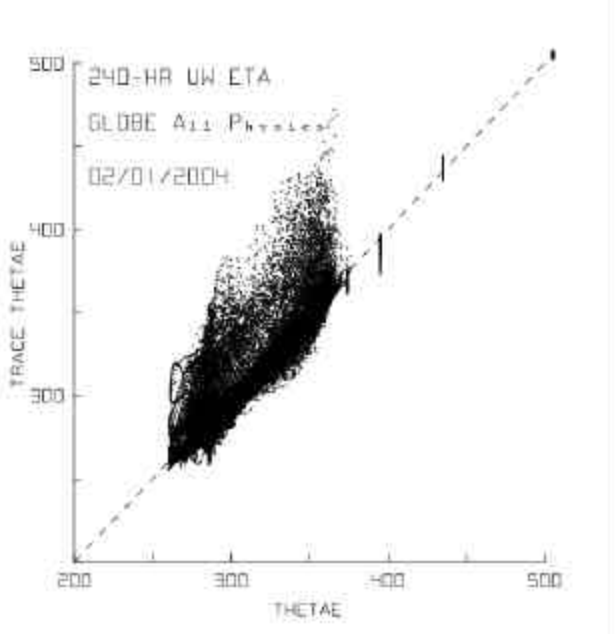

Dry

Large Scale condensation combined with Moist convective parameterization Moist Convection

Full Model

Non Conservation of trace of θ_e due to borrowing of mass

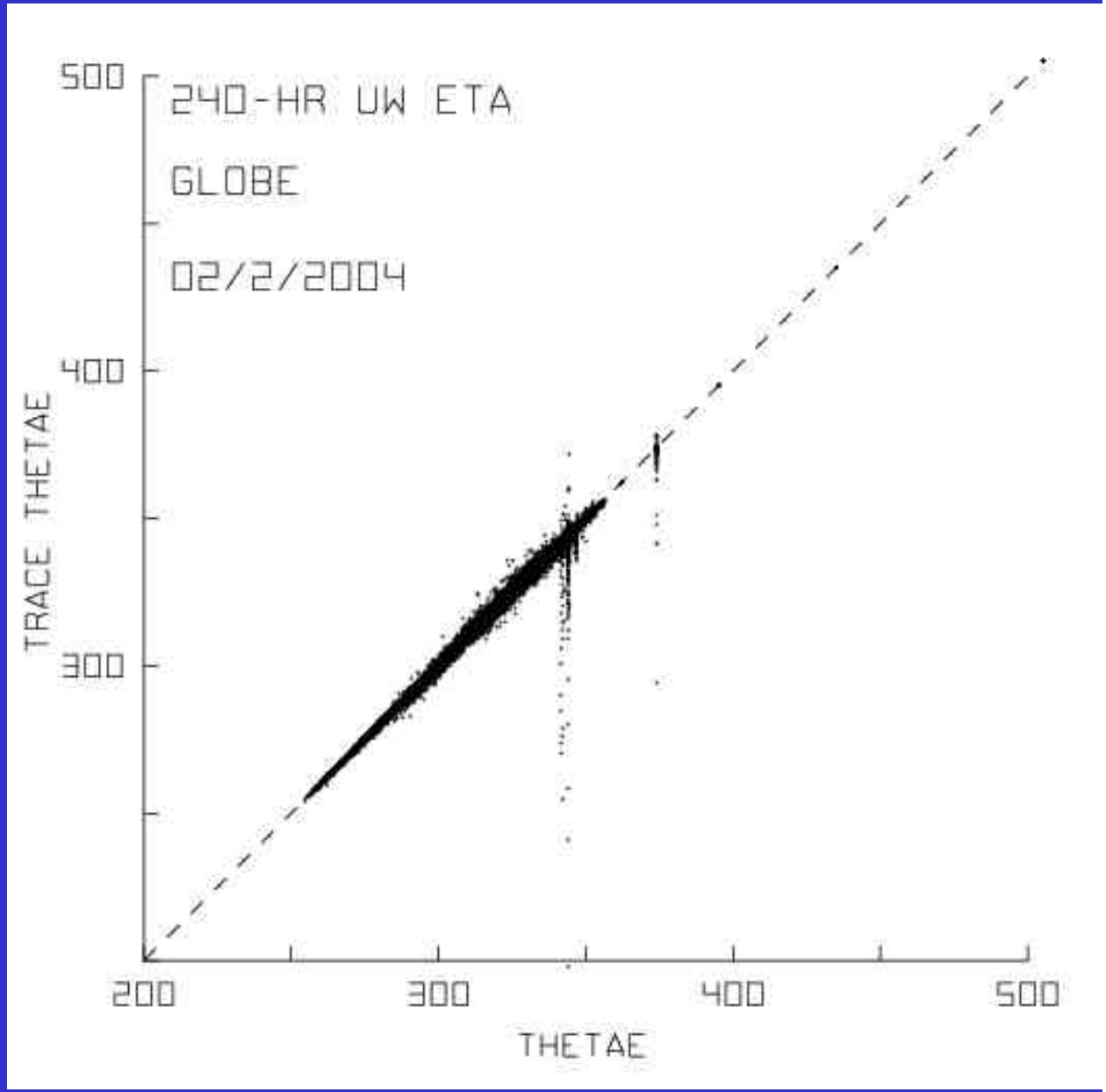

Bivariate Scatter and Relative Frequency Distributions and Vertical Profile of Mean Differences

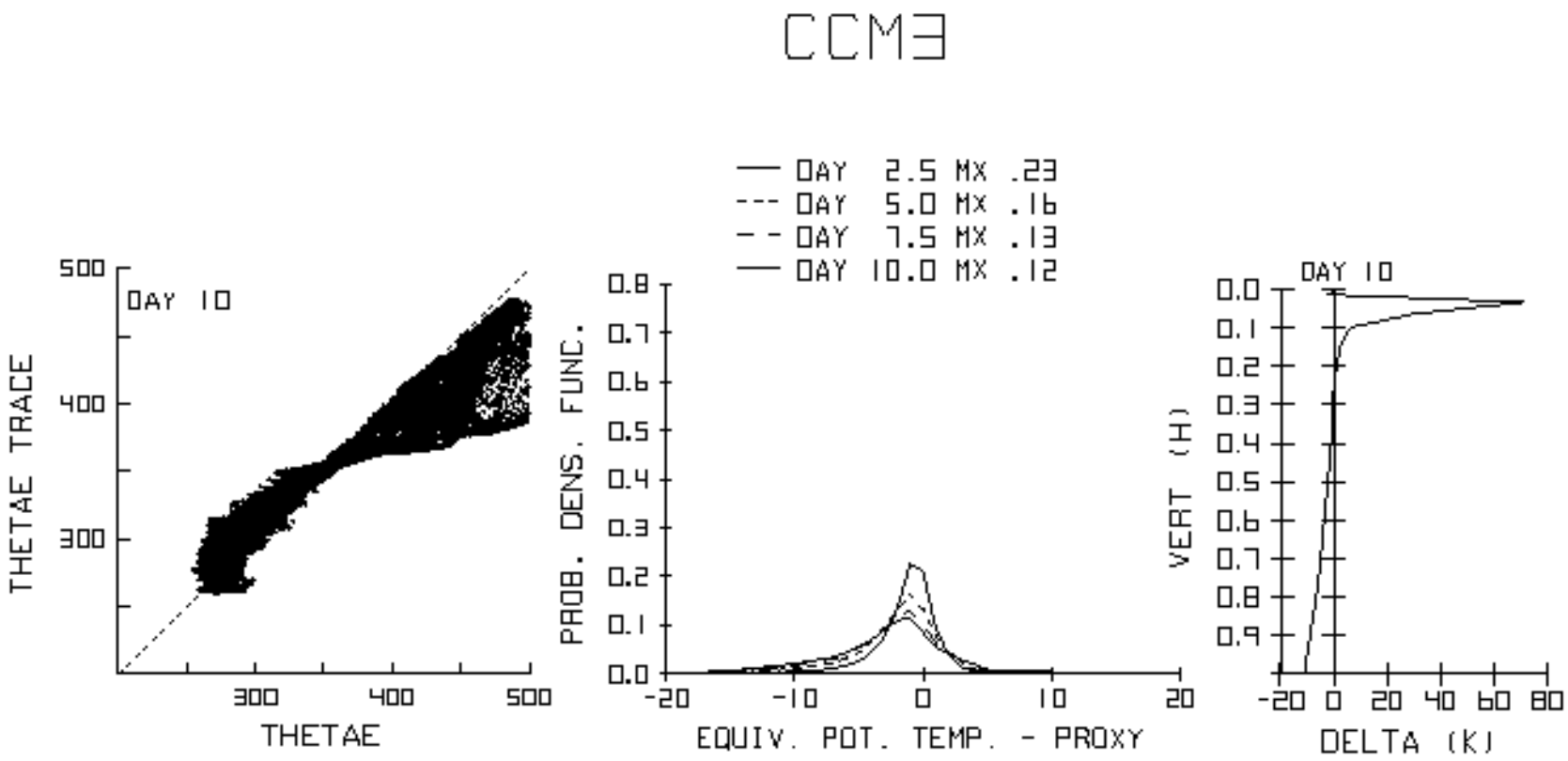

CCM3 Result Utilizing Weighted Overlapping Quadratic Polynomials

Bivariate distribution of θ_e and $t\theta_e$ from CCM3 utilizing linear combination of quadratic interpolants for q and $t\theta_e$ in lieu of Hermite cubic interpolants

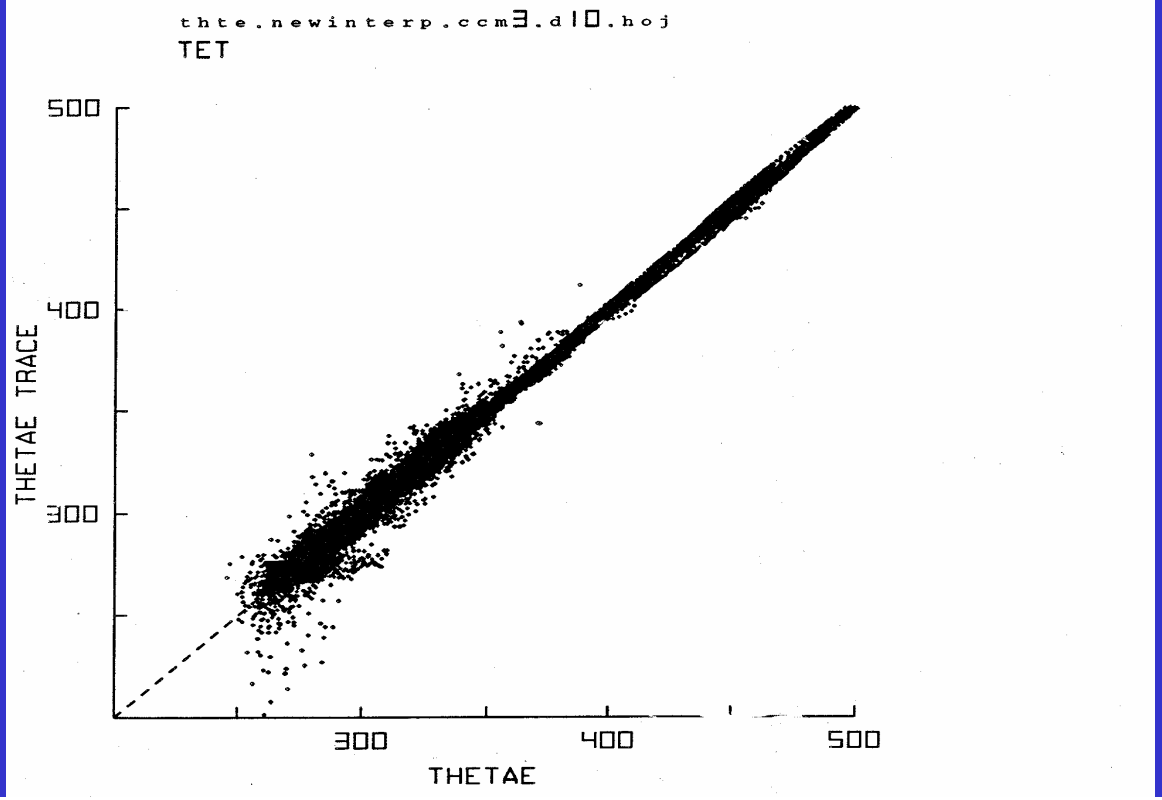

CCM3

	1-B		$A(\theta_e)$	$A(t\theta_e)$	$\hat{\delta}$		$\hat{\theta}_e$	$\hat{\theta}_e$	$\Delta\hat{\theta}_e$	
Layer/ Day	5	10	10	10	5	10	10	0	10-0	%Mass
5H	0.245	0.279	0.79	0.66	-0.8	-0.4	1124.3	1123.1	1.3	0.5
13H	0.147	0.120	1.31	2.29	-2.8	-2.5	782.7	782.5	0.3	1.4
33H	0.407	0.472	1.48	3.96	50.9	71.1	577.4	577.7	-0.2	2.8
64H	0.219	0.357	1.43	1.98	18.7	29.3	459.4	460.0	-0.5	3.5
99H	0.049	0.135	1.27	1.06	3.2	6.2	400.3	400.4	-0.2	3.5
139H	0.011	0.039	1.23	1.11	1.9	2.7	371.0	370.6	0.4	4.5
189H	0.033	0.052	1.03	1.02	0.9	1.3	351.1	350.2	0.9	5.6
251H	0.014	0.032	0.74	0.54	-0.1	0.0	338.1	336.5	1.5	6.8
325H	0.005	0.007	0.70	0.62	-0.4	-0.5	330.6	328.3	2.3	7.9
409H	0.005	0.007	0.63	0.57	-0.7	-1.0	325.8	323.2	2.6	8.9
501H	0.007	0.012	0.63	0.54	-1.4	-2.3	321.5	319.1	2.4	9.6
598H	0.011	0.020	0.67	0.54	-2.3	-3.6	318.3	315.6	2.7	9.8
695H	0.013	0.024	0.69	0.54	-3.2	-4.9	316.0	313.8	2.2	9.5
786H	0.015	0.024	0.77	0.62	-4.2	-6.3	314.0	312.4	1.6	8.7
866H	0.014	0.021	0.87	0.71	-5.6	-8.1	311.2	312.1	-0.9	7.2
929H	0.014	0.021	0.71	0.61	-6.4	-9.5	307.5	315.8	-8.3	5.3
970H	0.022	0.043	0.56	0.51	-7.1	-10.4	302.2	317.9	-15.8	2.9
992H	0.053	0.173	0.39	0.45	-7.2	-10.6	297.8	318.0	-20.1	1.5

Fig. 1A

CCM3 Modified

	1-B		$A(\theta_e)$	$A(t\theta_e)$	δ		$\hat{\theta}_e$	$\hat{\theta}_e$	$\Delta\hat{\theta}_e$	
Layer/ Day	5	10	10	10	5	10	10	0	10-0	%Mass
5H	0.231	0.275	0.75	0.79	0.78	0.66	1124.2	1123.1	1.1	0.5
13H	0.022	0.024	1.12	1.26	1.07	1.29	782.7	782.5	0.3	1.4
33H	0.021	0.025	1.37	1.43	1.69	1.79	577.5	577.7	-0.2	2.8
64H	0.006	0.006	1.29	1.40	1.39	1.49	459.5	460.0	-0.4	3.5
99H	0.003	0.003	1.16	1.23	1.22	1.31	400.4	400.4	-0.0	3.5
139H	0.004	0.004	1.08	1.17	1.12	1.18	371.0	370.6	0.4	4.5
189H	0.013	0.012	0.87	1.00	0.93	1.03	350.9	350.2	0.7	5.6
251H	0.006	0.007	0.87	0.79	0.91	0.83	337.7	336.5	1.2	6.8
325H	0.002	0.003	0.88	0.77	0.86	0.76	329.8	328.3	1.5	7.9
409H	0.002	0.003	0.80	0.68	0.79	0.68	325.1	323.2	1.9	8.9
501H	0.002	0.004	0.77	0.64	0.77	0.64	321.1	319.1	2.0	9.6
598H	0.004	0.005	0.77	0.65	0.76	0.63	318.0	315.6	2.4	9.8
695H	0.003	0.004	0.80	0.70	0.79	0.69	316.0	313.8	2.2	9.5
786H	0.004	0.005	0.83	0.75	0.82	0.73	313.8	312.4	1.4	8.7
866H	0.005	0.006	0.91	0.84	0.92	0.84	311.1	312.1	-1.0	7.2
929H	0.005	0.007	0.92	0.79	0.94	0.83	309.5	315.8	-6.3	5.3
970H	0.008	0.022	0.85	0.64	0.89	0.72	304.4	317.9	-13.6	2.9
992H	0.027	0.087	0.75	0.43	0.75	0.48	299.5	318.0	-18.5	1.5

A geometric perspective of the sums of squares of systematic differences relative to the equiangular line

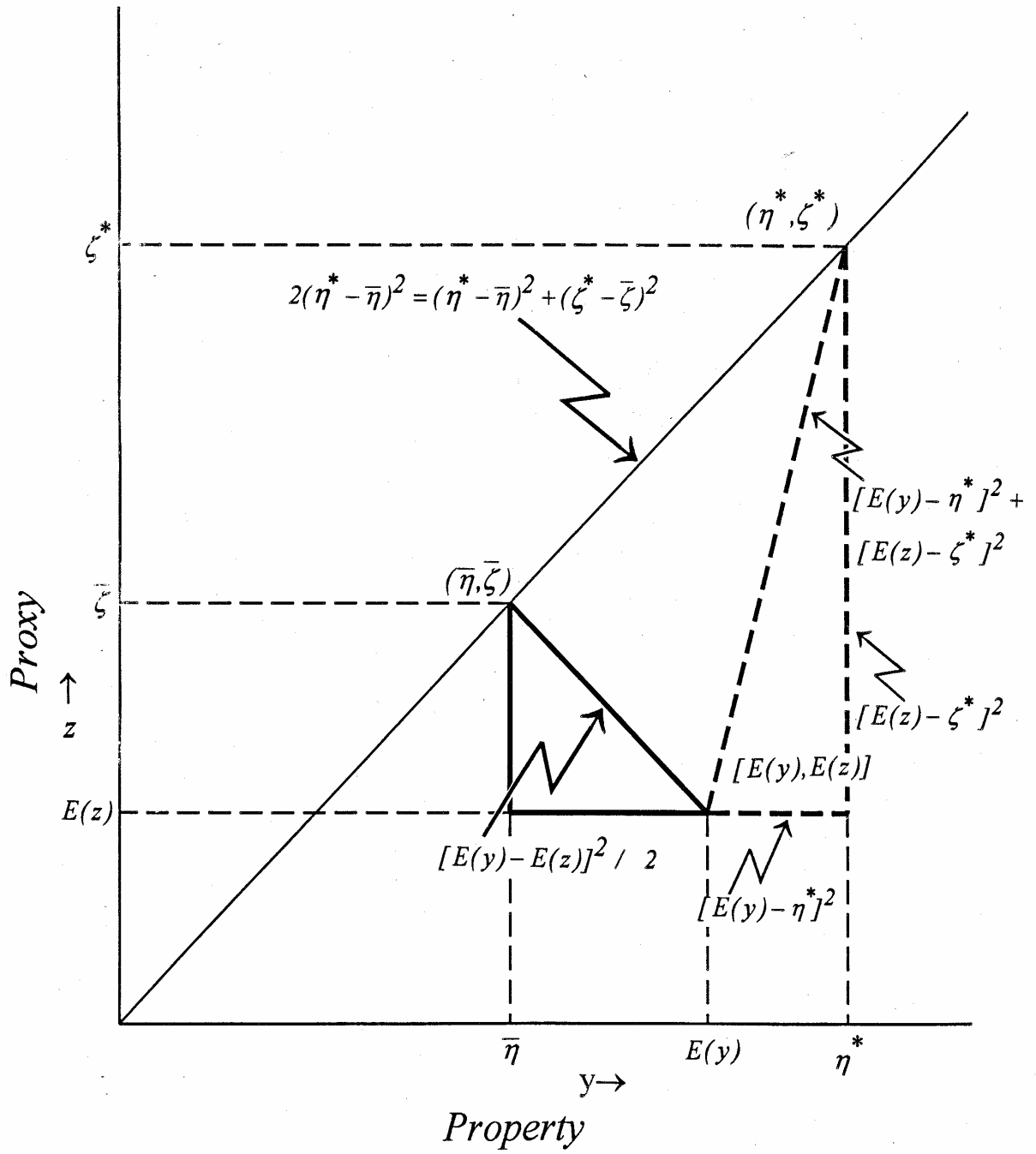

2. Validation of global and regional model simulations and also model assimilated data in relation to observed surface, radiosonde, satellite, aircraft and like measurements.

As part of this validation, both model simulated data and model assimilated data are compared against observations to assess how biases in the mean structure and spatial temporal variability of weather and climate models impacts assimilated data.

For weather models the validation involves instantaneous and temporal comparisons with in situ and remotely sensed observations to determine forecast error spatially and temporally.

For climate models, the validation involves comparison of simulated distributions corresponding with observed distributions; the form and modal nature of the distributions, measures of variation including second and higher order moments, etc.

The key thrusts of both are to assess and determine reasons for model drift and resulting biases spatially and temporally for both model simulated and assimilated data relative to the actual atmosphere; --- numerics, filtering, sub grid scale parameterizations, numerical and physical dissipation, selective numerical damping, non linear interactions, orography, deficiencies in resolving scale dependency and diurnal forcing of dry and moist convection including interaction with solar and infrared radiation, etc. Here temporally averaged vertical profiles of diabatic and other processes including vertically integrated distributions of the various simulated processes over different geographical regions provide relevant information for the comparisons.

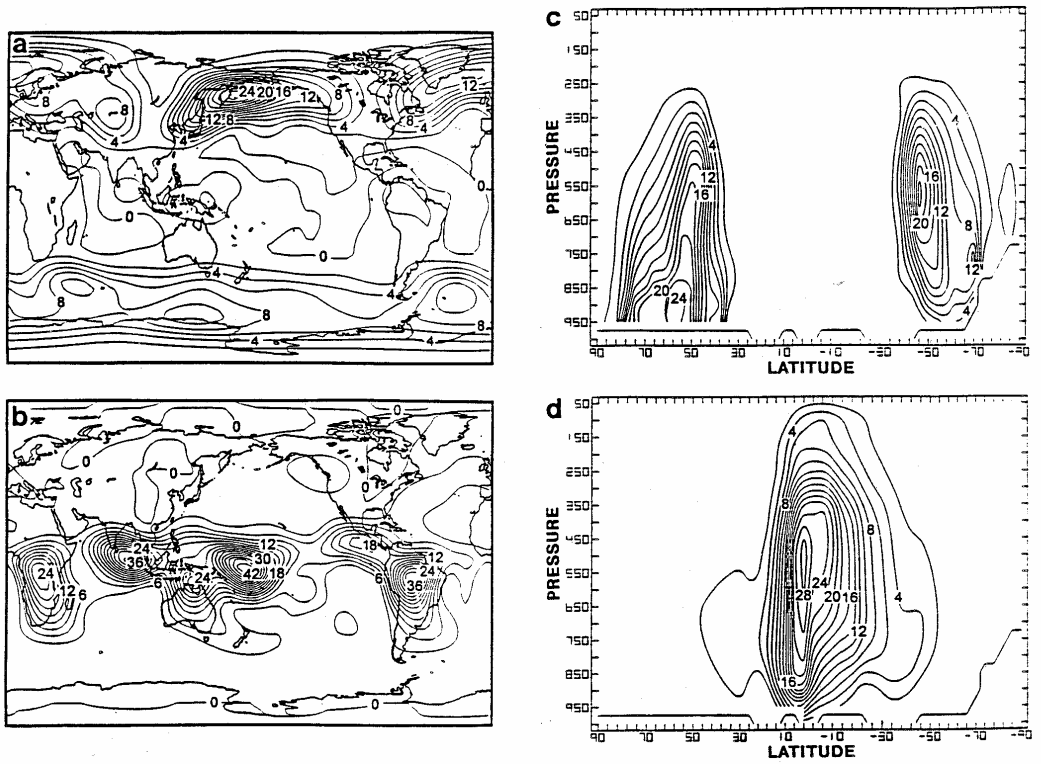

Fig. 5. Temporally averaged (a) large-scale heating and (b) convective heating, and temporally and zonally averaged (c) large-scale heating and (d) convective heating for DJF 1995 from a 137-day UW θ–σ model simulation. All units 0.1 K day^{-1}.

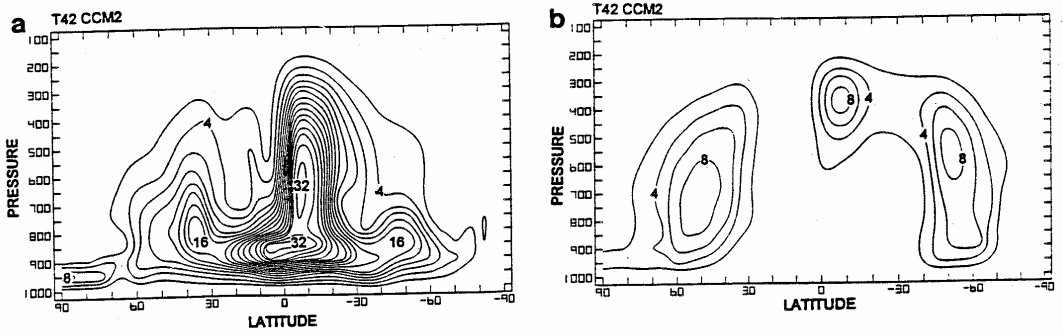

Fig. 6. The temporally and zonally averaged (a) convective heating and (b) large-scale heating for ten Januarys from a CCM2 climate simulation. All units 0.1 K day^{-1}.

Zonally Averaged Clouds (%)

McRAS

CCM3

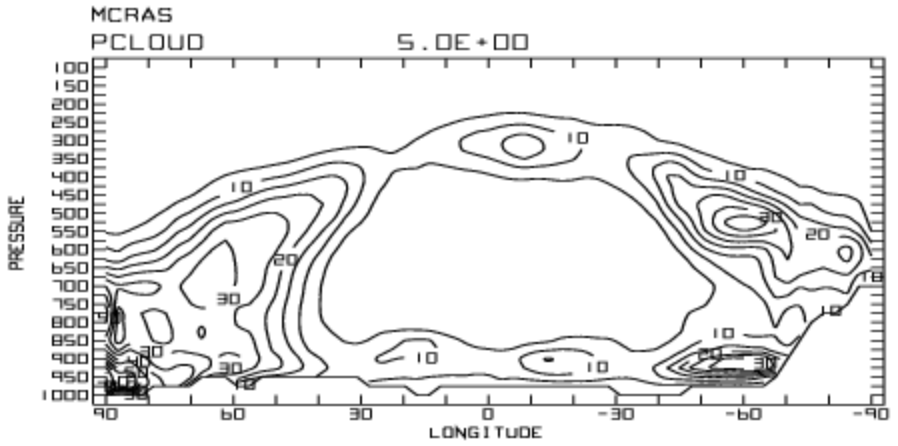

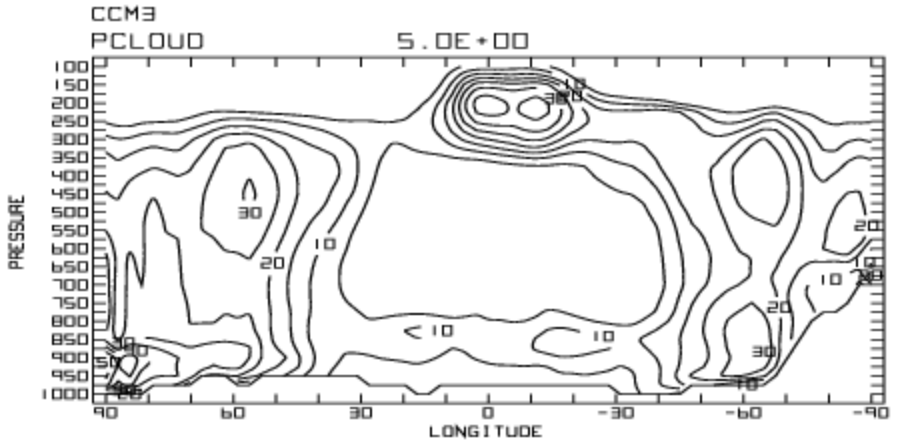

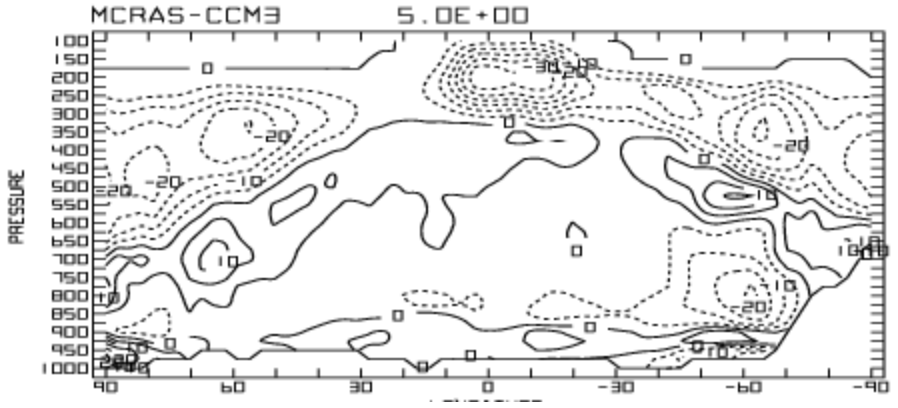

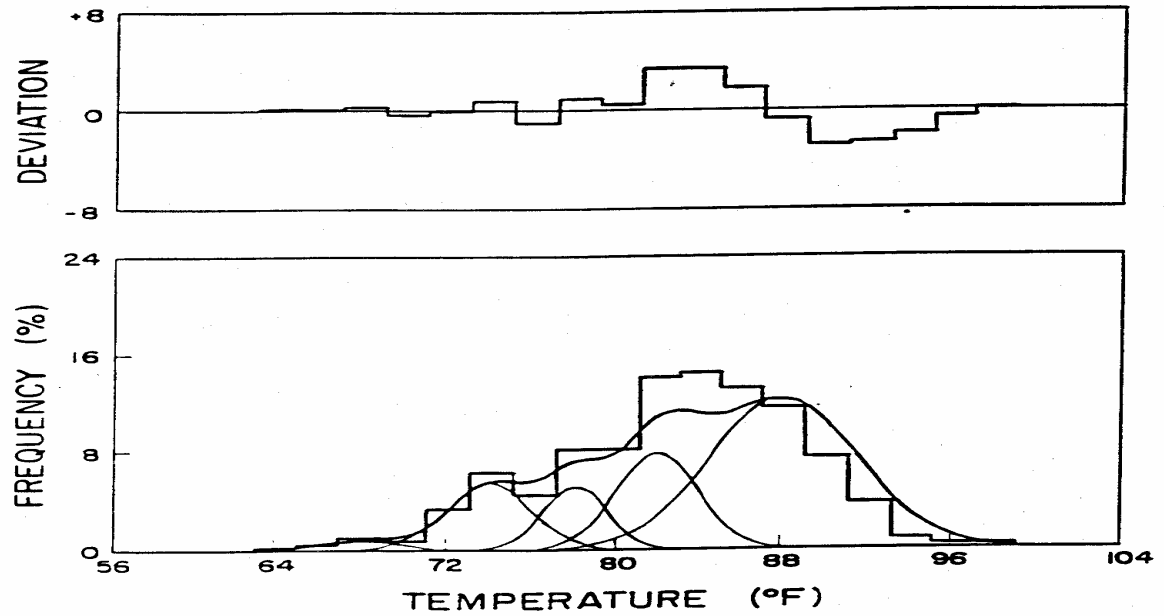

Figure 2. Observed probability histogram and the results of the partial collective model graphical estimates for Pittsburgh, Pa.

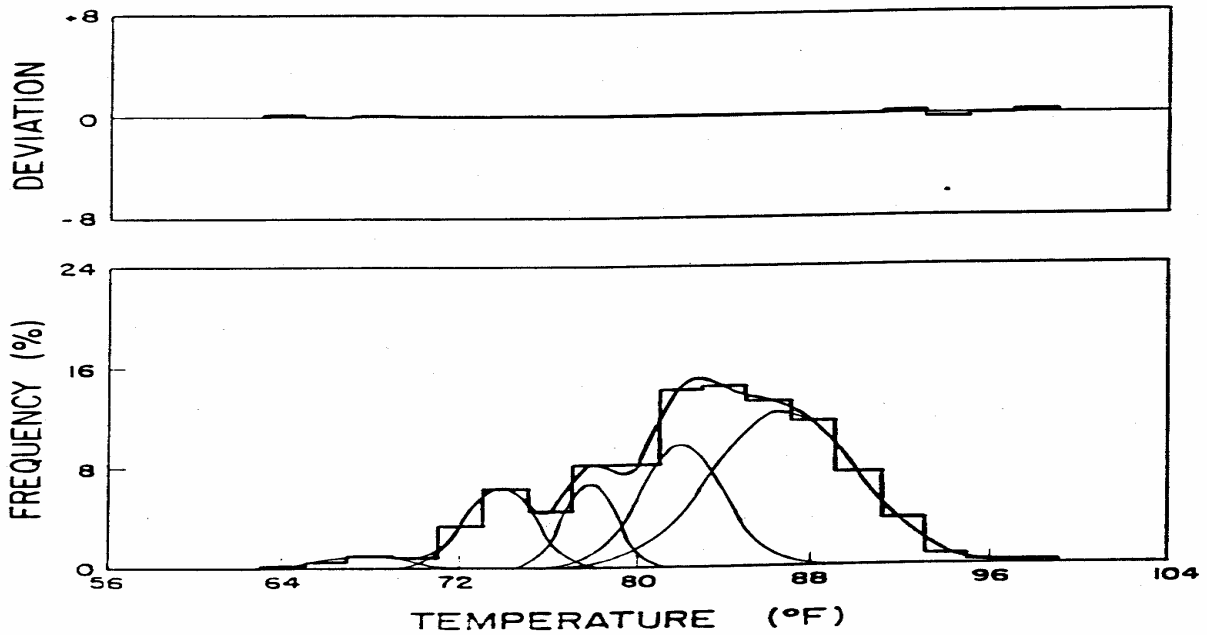

Figure 3. Least squares estimates of the partial collective parameters for Pittsburgh, Pa.

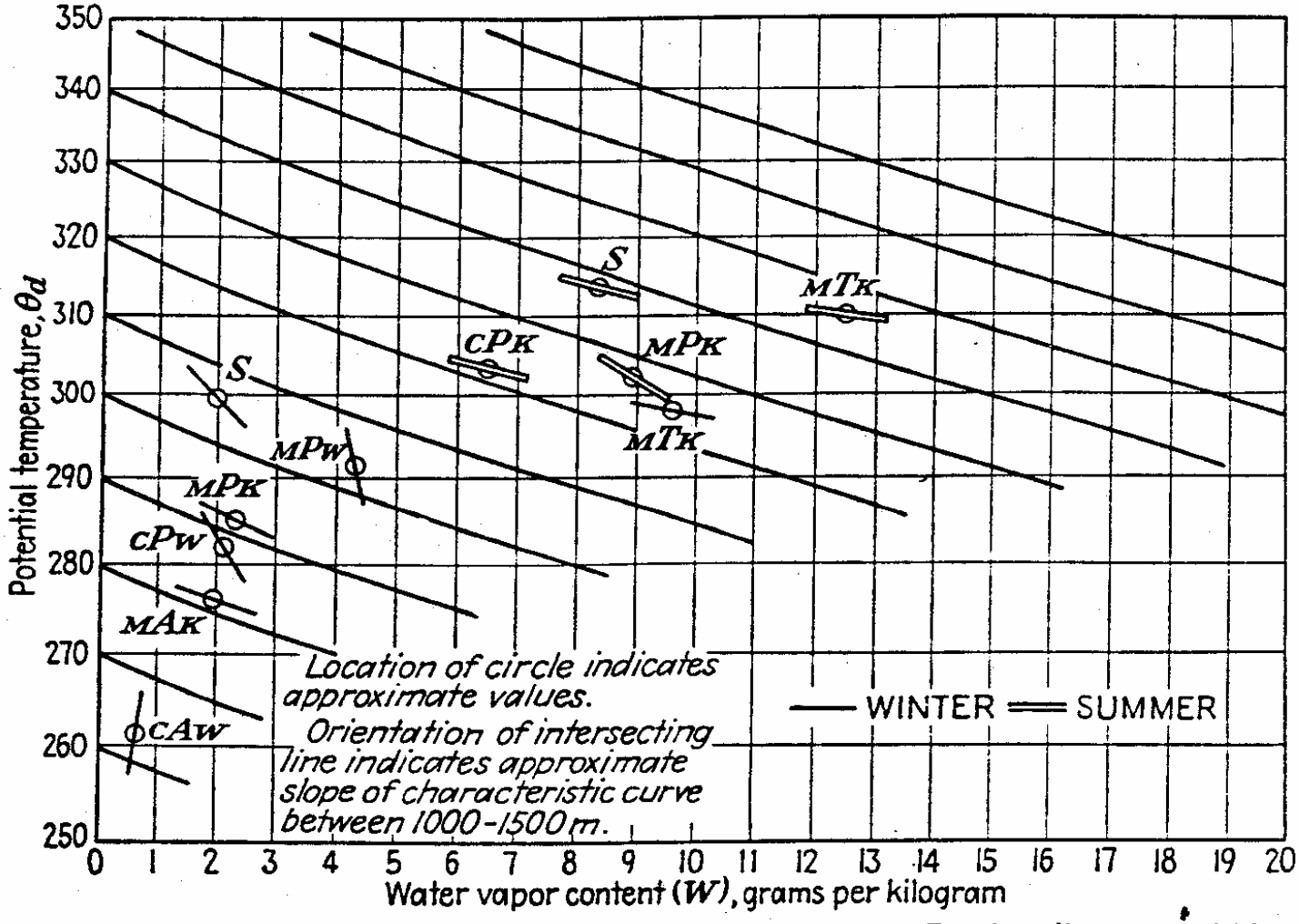

FIG. 3.—Identification of North American air masses on a Rossby diagram. (*After Showalter.*)

Figure 4. Identification of North American air masses on a Rossby diagram. (After Showalter.) (From Berry and Ballay 1945)

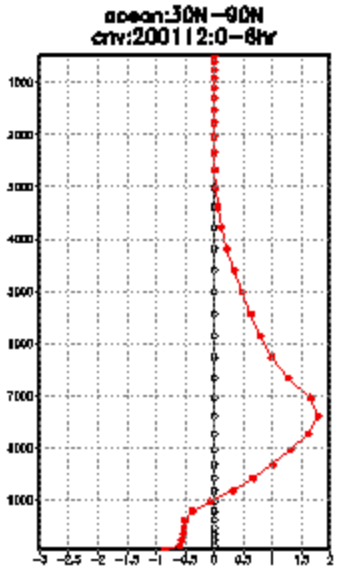
ocean:30N-90N
cnv:200112:0-6hr

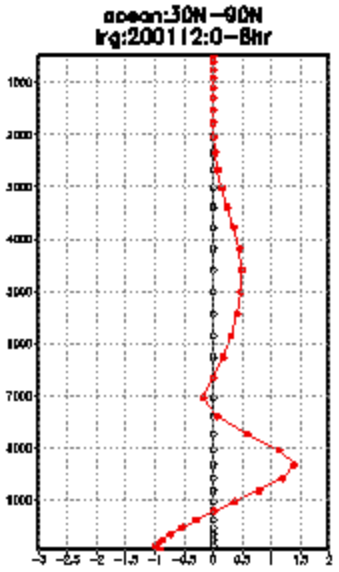
ocean:30N-90N
lrg:200112:0-6hr

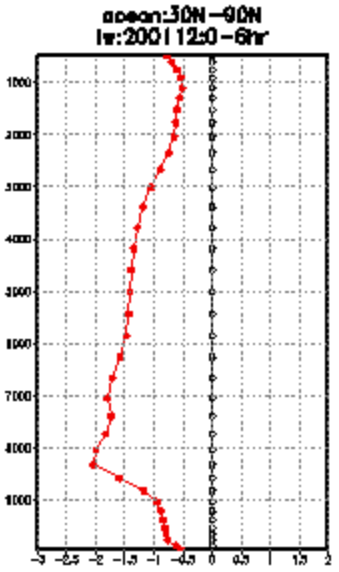
ocean:30N-90N
lw:200112:0-6hr

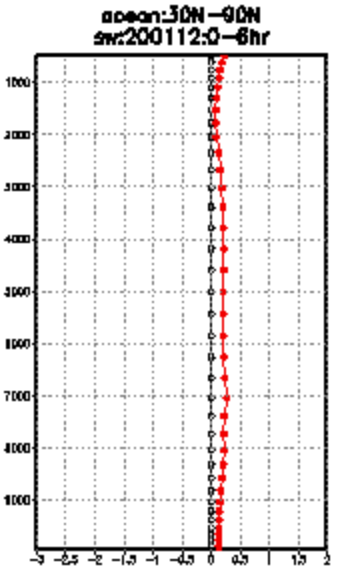
ocean:30N-90N
sw:200112:0-6hr

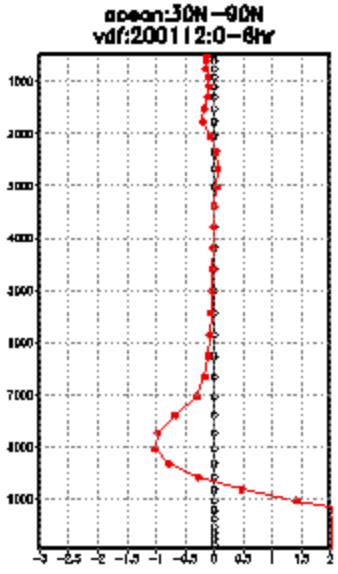
ocean:30N-90N
vdf:200112:0-6hr

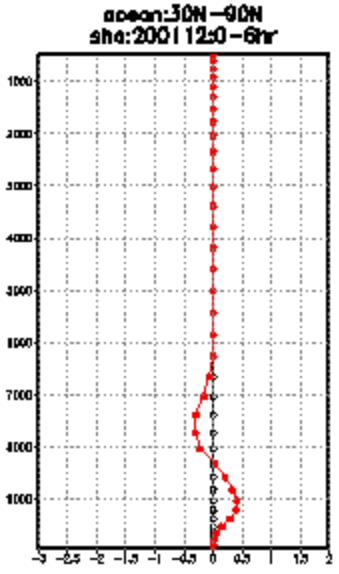
ocean:30N-90N
sha:200112:0-6hr

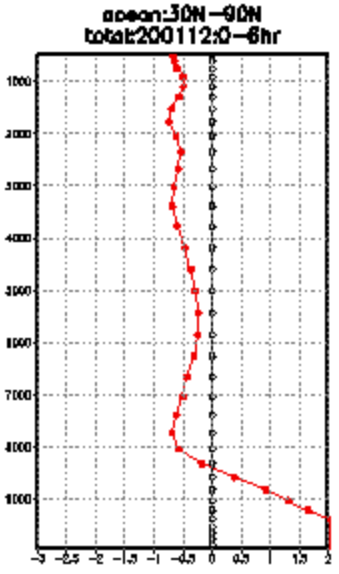
ocean:30N-90N
total:200112:0-6hr

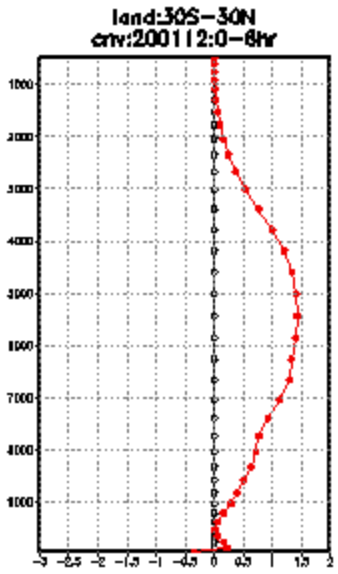
land:30S-30N
cnv:200112:0-6hr

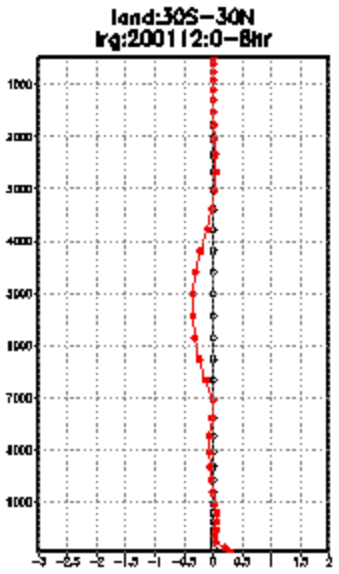
land:30S-30N
lrg:200112:0-6hr

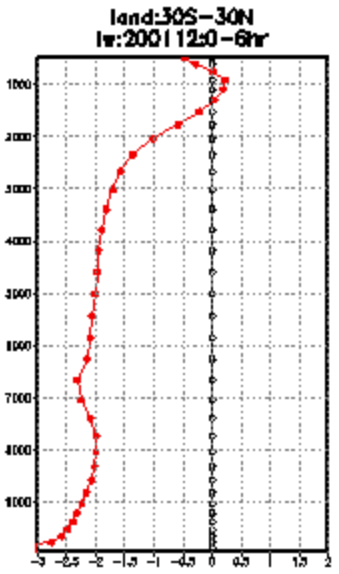
land:30S-30N
lw:200112:0-6hr

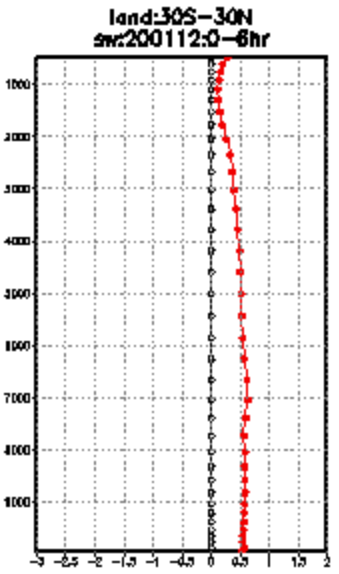
land:30S-30N
sw:200112:0-6hr

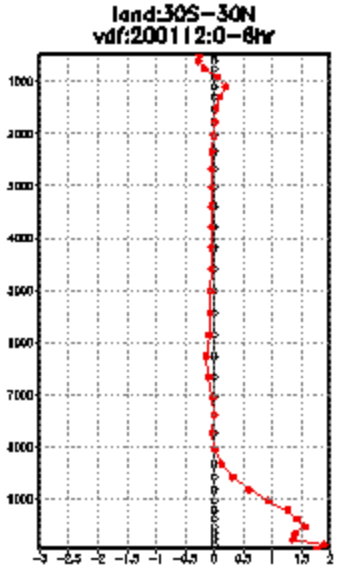
land:30S-30N
vdf:200112:0-6hr

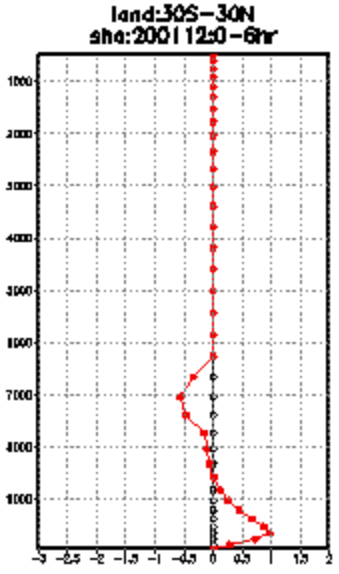
land:30S-30N
sha:200112:0-6hr

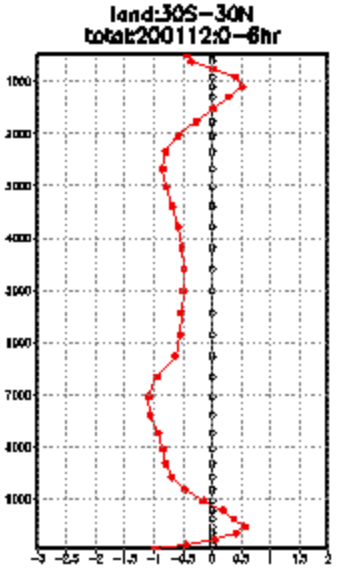
land:30S-30N
total:200112:0-6hr

3. Comparative analyses of the global distribution of proxy water vapor brightness temperatures calculated from model simulated profiles of temperature, pressure and mixing ratio using forward radiance models versus observed satellite brightness temperatures

The comparison of the model's simulated water vapor brightness temperatures as determined by forward irradiance calculations is to assess drift of a model's simulated water vapor distribution from reality for both weather and climate models. For weather models the comparison involves an instantaneous comparison with the corresponding satellite observation. For climate models, the comparison involves temporally averaged water vapor brightness temperatures as simulated versus corresponding temporally averaged satellite measurements over different seasons, different regions and different periods of simulations.

Similarly the temporally averaged global distribution of a climate model's simulated upwelling irradiance within spectral intervals critical to the determination of the vertical distributions of temperature and the spatial distributions of other radiatively active constituents should be compared with the corresponding temporally averaged observed spectral distribution of radiation by satellites.

4. Diagnostics of transport equations in model coordinates, sigma, isentropic, hybrid sigma isobaric, hybrid isentropic sigma coordinates – mass, angular momentum, energy, water vapor, atmospheric constituents, etc.

The following lists capabilities for diagnostics of transport processes that are embodied within the governing equations of weather and climate models. For maximum insight and accuracy in the determination of a model's simulation of the Eulerian components of transport and also Lagrangian sources and sinks of properties, the diagnostics should be carried out in the coordinate system employed in the model. Direct diagnostic comparisons of corresponding global simulations from model to model are only valid in general with integration over the entire vertical extent of a model's atmosphere.

a. Transport components, zonal mean and eddy, temporal standing and transient, combination of zonal and temporal components.

b. Lagrangian sources/sinks computed directly or estimated as a residual from evaluation of the transport equation for a property.

c. State structure, vertical averages, zonal averages, vertical-zonal averages, global averages, averages over regional domains, averages over arbitrary space and time.

d. Water vapor – P-E (precipitation minus evaporation), residence times, global, tropics, extratropics, continental domains, ocean basins, arbitrary regions.

Within these comparisons, it is essential to recognize the condition that the individual terms of the Eulerian expansion of the Lagrangian source of atmospheric properties are not invariant, that is, the tendency and divergence as simulated differs from model to model depending on the particular coordinate system employed in the representation of the governing equations. In addition, recognition must be made that the transfers of momentum and of energy across temporally and spatially varying inclined quasi-horizontal coordinate surfaces by pressure viscous stresses and by work, respectively, are coordinate dependent processes.

In the comparison of the vertical integral of the governing equations among global simulations for both weather and climate, efforts should be made to ascertain a given model's capabilities to globally conserve mass, momentum, total energy [kinetic, gravitational potential, and internal (including latent energy of phase changes)] and other constituents in relation to boundary fluxes. Discrepancies between the vertical integral of the interior transport of properties and the boundary fluxes are likely sources of bias and random errors within the model simulated atmosphere.

Beside the potential sources of error just noted, there is the issue of a model's capability to simulate reversibility of thermodynamic processes associated with transformations among the various components of total energy that is demanded from entropy principles in terms of dry and moist adiabatic processes internal to the atmosphere.

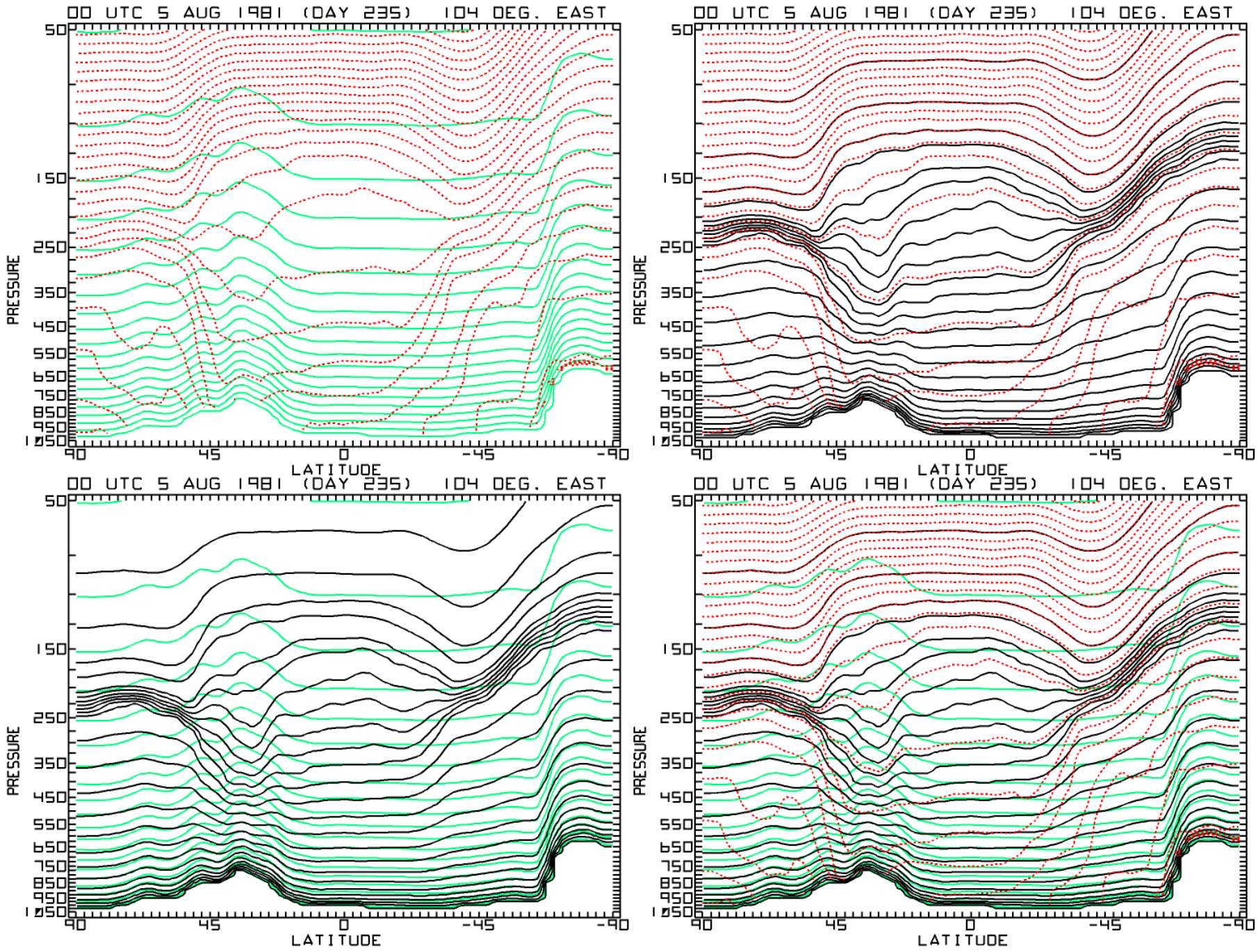
00 UTC 5 AUG 1981 (DAY 235) 104 DEG. EAST
PRESSURE
50
150
250
350
450
550
650
750
850
950
1050
90
45
0
-45
-90
LATITUDE
00 UTC 5 AUG 1981 (DAY 235) 104 DEG. EAST
PRESSURE
LATITUDE
00 UTC 5 AUG 1981 (DAY 235) 104 DEG. EAST
PRESSURE
LATITUDE
00 UTC 5 AUG 1981 (DAY 235) 104 DEG. EAST
PRESSURE
LATITUDE

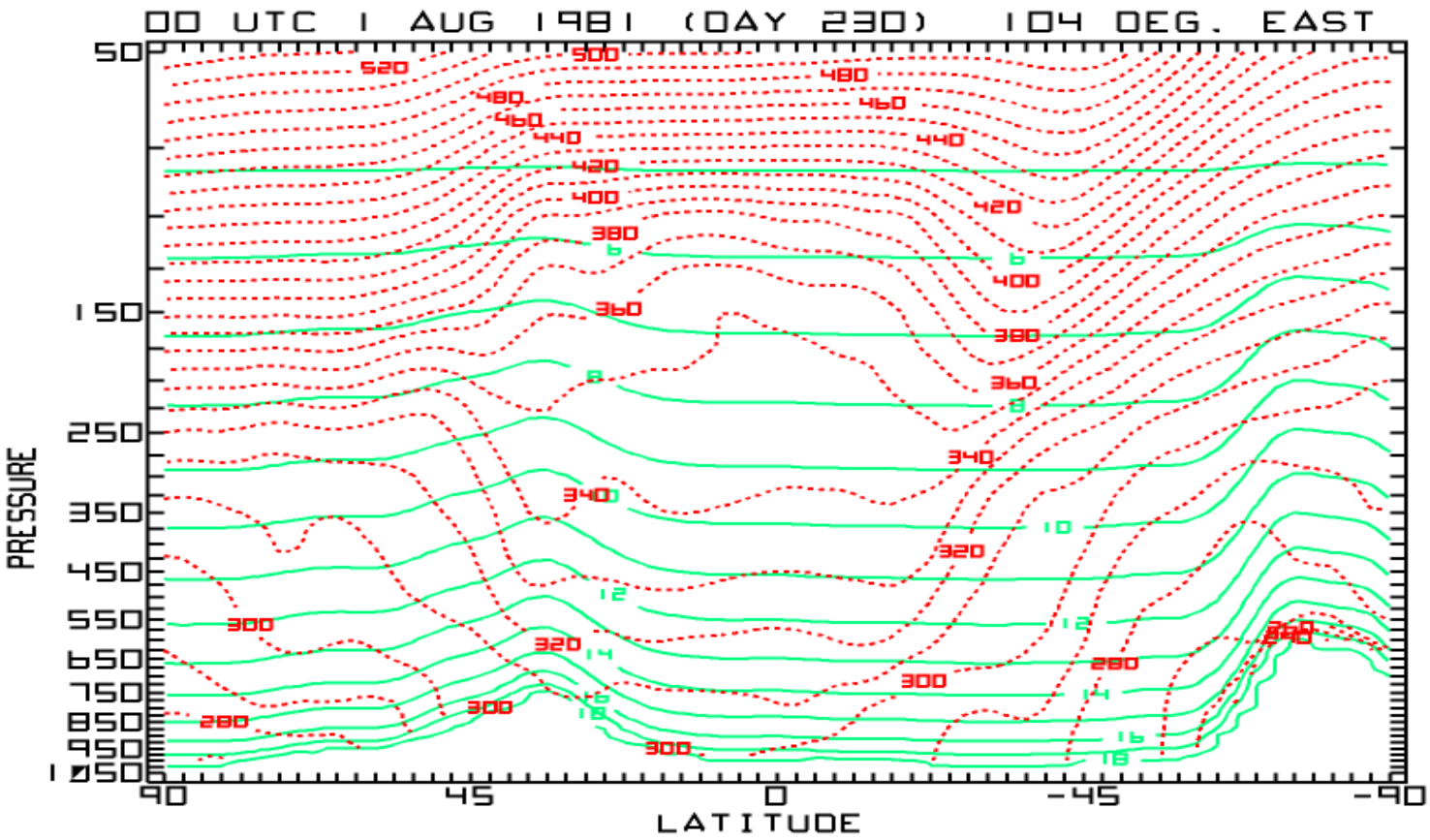
00 UTC 1 AUG 1981 (DAY 230) 104 DEG. EAST
PRESSURE
50
150
250
350
450
550
650
750
850
950
1050
90
45
0
-45
-90
LATITUDE
520
500
480
460
440
420
400
380
360
340
320
300
280
6
8
10
12
14
16
18

Regional Air Quality Modeling System (RAQMS)

UW - NASA Langley

RAQMS is a meteorological and chemical modeling system for assimilating remote and in-situ observations of atmospheric chemical composition and predicting the distribution of atmospheric trace gases (air quality).

- UW Hybrid Global Model (UW θ-η)
- Non Hydrostatic Modeling System (UW-NMS)
- NASA Langley - LaRC Interactive Modeling Project for Atmospheric Chemistry and Transport Model

Ozone assimilation- ECMWF meteorological fields
HALOE, POAMS, SAGE ozone observations
6 hour intervals

TOMS

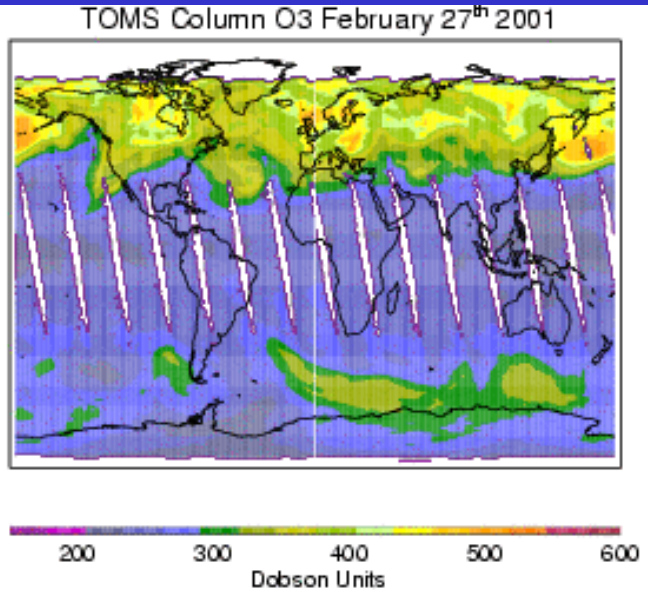

Day 15 of assimilation

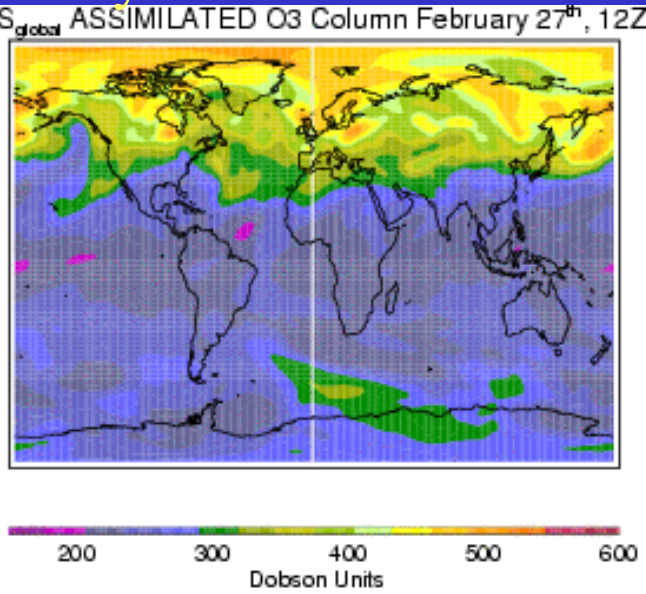

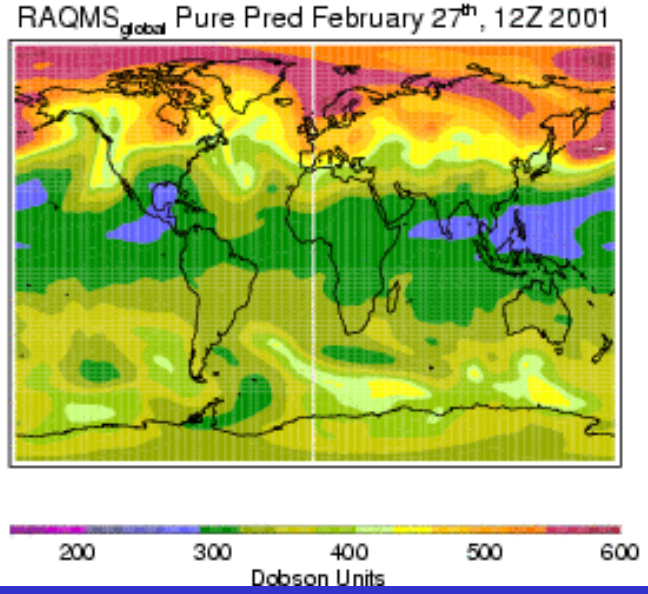

Assimilating 3-d observations of ozone from HALOE, SAGE and POAMS satellite platforms.

Column Integrated Ozone 12Z February 27, 2001.

Day 15 of simulation where Ozone is forecast

5. Three-dimensional distributions of the Lagrangian sources of entropy expressed as potential temperature change in degrees per day or specific heat addition determined from diagnostics employing the isentropic mass continuity equation.

a. Vertically averaged throughout the atmosphere

b. Layered and vertically averaged over specific layers

c. Zonal and temporally zonal averaged

d. Vertical profiles

e. Regionally averaged vertical profiles over continents, ocean basins, and subdomains of continents and oceans representative of different climate regimes

f. Arbitrary time and space domains or combinations there of

6. Compare estimates of the Lagrangian sources of entropy diagnosed from assimilated data, first guess fields and model predicted heating from medium range, subseasonal and seasonal forecasts in accord with 5 above.

7.Determine rotational/irrotational components of transport of mass, energy, entropy, water vapor and constituent atmospheric properties by layer or arbitrary combination of layers by vertical integration.

One key purpose of this diagnostic transport calculation is to study the role of the temporally averaged mass transport in the long range transport of atmospheric properties in relation to the systematic sources of entropy by differential heating within monsoons.

In isentropic coordinates, the systematic transport is global in extent, in other coordinates, the transport being by ageostrophic motion is more or less restricted to the tropics/subtropics.

8. Mean meridional zonally averaged mass circulations and their forcing in accord with Eliassen's concepts as determined for isobaric, sigma, isentropic, model, and hybrid model coordinates with partitioning into geostrophic and ageostrophic components

For details concerning the generalized form of transport equations appropriate for the governing equations of atmospheric models discussed herein, see Johnson, D. R., 1980: A Generalized Transport Equation for Use in Meteorological Coordinates Systems. Monthly Weather Review, 108, 733-745.

9. Additional considerations

While the emphasis has been on carrying out diagnostic assessments in the coordinate system of a model to preclude vertical interpolation errors, the generalized diagnostic capabilities described heretofore include the capability to interpolate the state structure of fields from one model coordinate system to another, as well as the capability to interpolate to isobaric coordinates. Traditionally diagnostic studies of the general circulation have been conducted in isobaric coordinates, and as such the 4DDA data sets from reanalysis and assimilation for medium range weather prediction include expression in isobaric coordinates to facilitate comparisons. Such comparisons are needed and deserve to be continued. Certain difficulties emerge however in determination of the accuracies of a given model. The most obvious is the difficulty that state variables and boundary exchange processes of the various forms of energy and atmospheric constituents as well as the transfer of momentum by pressure viscous stresses at the earth/atmosphere interface are not accurately specified by the isobaric representation. Neither are the state structure and energy fluxes at the model's upper boundary prescribed adequately. Then there are the difficulties that vertical interpolation errors negate the accuracies needed for assessment of pure error in the determination of conservation of moist and dry entropies.